



# Oligocene-Miocene sequence stratigraphy in the northern margin of the South China Sea: An example from Taiwan

Andrew T. Lin<sup>a,\*</sup>, Chih-Cheng Yang<sup>b</sup>, Ming-Huei Wang<sup>c</sup>, Jong-Chang Wu<sup>b</sup>

<sup>a</sup> Department of Earth Sciences, National Central University, Taiwan

<sup>b</sup> Exploration and Production Business Division, CPC Corporation, Taiwan

<sup>c</sup> Exploration and Development Research Institute, CPC Corporation, Taiwan

## ARTICLE INFO

### Keywords:

Passive continental margin  
Sequence stratigraphy  
South China Sea  
Taiwan

## ABSTRACT

Oligocene-Miocene sediments in the Taiwan region were accumulated in the NE passive-continental margin of the South China Sea. We utilized around ~200 boreholes and reflection seismic data to study the Oligo-Miocene sequence stratigraphic framework in the Taiwan region. Major sequence boundaries are used to map out various sediment isopach maps, enabling us to decipher dominant tectonic events during the course of passive-margin evolution.

The Oligocene-Miocene succession is divided into 16 sequences on the basis of well-log correlation. These 16 sequences can be grouped into four (A, B, C, D) sequence sets. Isopach maps of sequence sets B and C (~21–12.5 Ma) show that they blanket the west Taiwan basins with relatively uniform thickness deposited during uniform and slow basement subsidence. Sequence sets A (~30–21 Ma) and D (~12.5–6.5 Ma), however, thickened into fault-bounded troughs, recording two extensional events that were especially active in the outer margin (i.e., the Tainan Basin). There is a general correlation between the Taiwan Miocene sequences and the glacioeustasy during the interval ~21–6.5 Ma. Therefore, eustasy is the dominant control on the Taiwan Miocene stratigraphic development. The deposition of the sequence set A during ~30–21 Ma and possibly the sequence set D in the outer margin during the late Miocene, however, appears to have been strongly modulated by extensional tectonics and local sedimentary factors (e.g., rates of basin subsidence, sediment supply and basin physiography, etc.).

## 1. Introduction

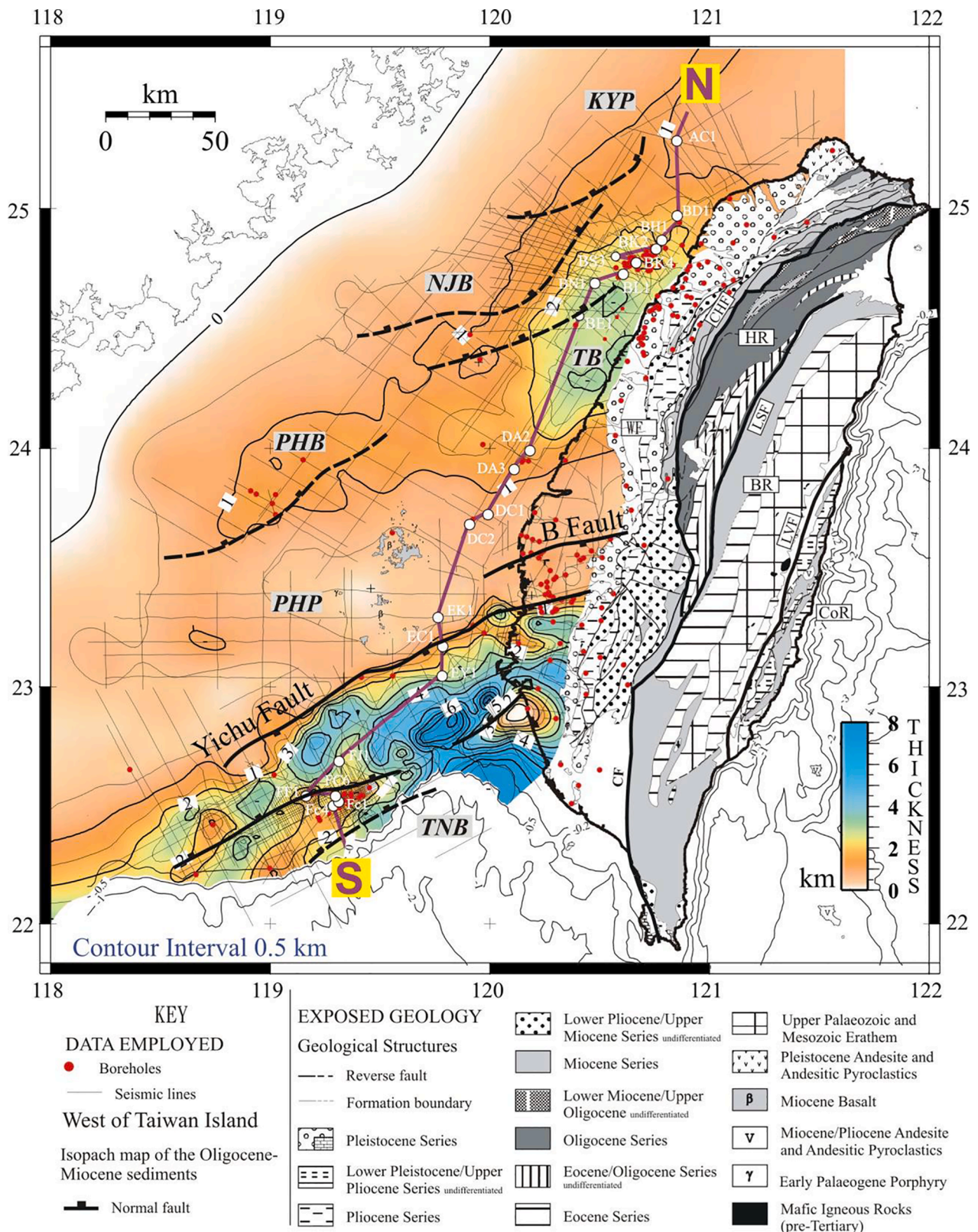
The Oligocene-Miocene siliciclastic sedimentary succession in the Taiwan region was deposited in various sedimentary basins in the northern passive margin of the South China Sea. This succession was accumulated after the initiation of the seafloor spreading of the South China Sea since the middle Oligocene (Briaies et al., 1993) and prior to the collision between the Luzon volcanic arc and the passive continental margin since the late Miocene (Teng, 1990; Teng and Lin, 2004), which turned the study area into a foreland basin (Lin et al., 2003).

Fig. 1 shows the sediment thickness for the studied Oligocene-Miocene sediments in the Taiwan Island as well as in the Taiwan Strait. The studied sediment succession is accumulated in a passive margin that experience two episodes of rifting during ~30–21 Ma, and 12.5–6.5 Ma, respectively, with an intervening tectonic quiescence stage during 21–12.5 Ma, dominated by thermal subsidence (Lin et al., 2003).

Assuming constant rate of sediment supply, during thermal-subsidence stage, eustasy would be the major governing factor on sedimentation as the case seen in the Atlantic New Jersey margin (Miller et al., 1998; Browning et al., 2013), whereas during rifting stage, extensional tectonics may play an important role on sediment architecture (Ravnas and Steel, 1998; Martins-Neto and Catuneanu, 2010; Holz et al., 2017). The studied succession is of fluvial, coastal, to shallow marine origin and hence sensitive to changing eustatic sea-levels, sediment supplies and climates. Therefore, the Taiwan Oligocene-Miocene succession provides with us a rare opportunity to unravel the governing factors, such as rifting tectonics, global sea-level, climate, and local sediment supply on the architecture of sedimentary successions. We address this problem by a detailed sequence stratigraphic analysis using well logs and seismic data with age constraints from nannofossil biostratigraphic zones.

Sequence stratigraphic approach is successfully and widely applied in many siliciclastic passive margins, with the New Jersey margin being

\* Corresponding author at: Department of Earth Sciences, National Central University, Taiwan, 300 Jungda Road, Chungli, Taoyuan 32001, Taiwan.  
E-mail address: [andrewl@ncu.edu.tw](mailto:andrewl@ncu.edu.tw) (A.T. Lin).



**Fig. 1.** Regional geology and data used in the study. The isopach of the Oligocene-Miocene sediments (Lin et al., 2003) is shown as a color-shaded map with contour lines shown in km. Thick black lines on this isopach map are major normal faults with continuous lines indicating that faults cut through the Oligocene-Miocene strata, and dashed lines indicates faults buried beneath the studied stratigraphic sections. Borehole data are shown as red and filled circles, and seismic lines are shown as thin black lines. The white circles connecting by a thick purple line are boreholes with names shown in well-log correlation panels of Figs. 7, 10, 12, 14. The onshore geology is from Ho (1988). Abbreviations: BR: Backbone Range, CHF: Chiuchih Fault, CF: Chaochou Fault, CoR: Coastal Range, HR: Hsuehshan Range, KYP: Kuanyin Platform, LSF: Lishan Fault, LVF: Longitudinal Valley Fault, NJB: Nanjihtao Basin, PHB: Penghu Basin, PHP: Penghu Platform, TB: Taihsi Basin, TNB: Tainan Basin, WF: Western Foothills. (For interpretation of the references to color in this figure legend, the reader is referred to the web version of this article.)

the prime example (e.g., Browning et al., 2008, 2013). Spatial correlations on stratal surfaces within sequences provide a chronostratigraphic framework for basin sediments. Sequence approach therefore holds an opportunity to correlate different lithostratigraphic units among different basins for sediments showing pronounced lateral facies change such as the case for the studied Taiwan sediments. The sediment packets bounded by major sequence boundaries, which are of regional chronostratigraphic significance (e.g., Catuneanu, 2017), can then be mapped out to generate sediment isopach maps to infer depositional and tectonic factors shaping the sediment architectures.

The sequence stratigraphic analysis presented here is based largely on data from ~200 boreholes supplemented by seismic reflection data. Seismic data are also used to determine sediment thickness for major sequence sets (see Section 6) in addition to borehole data. The datasets of boreholes and reflection seismic profiles are the same as that presented and used in Lin et al. (2003). The work of Lin et al. (2003) does not present a detail borehole sequence stratigraphic framework, however. The objectives of this work are therefore (1) to establish an interbasinal sequence stratigraphic architecture and a chronostratigraphic framework; (2) to construct sediment isopachs that correspond to different tectonic phases during the Oligocene-Miocene post-breakup episode; (3) to correlate the Taiwan Oligocene-Miocene sequence to “global” signatures of oxygen and carbon isotopes, sea levels, and climates; and (4) to unravel the governing factors that shape the sediment

architectures in the South China passive margin.

## 2. Stratigraphic framework and previous studies

The Taiwan Oligocene-Miocene succession can be broadly grouped into two regions, to the north and to the south of the Penghu Platform, respectively, according to overall sediment geometry and lithology (Fig. 1). To the north of the Penghu Platform, Oligocene-Miocene strata comprise a shale/sandstone sequence that deposited in continental to shallow-marine environments. This sequence was laid down above the Eocene, Paleocene or older rocks and thickened over preceding syn-rift depocenters and onlapped toward adjacent basement highs. In contrast, to the south of the Penghu Platform, in the fault-bounded Tainan Basin, a several kilometers-thick, Miocene marine mudstone sequence floored by an Oligocene basal transgressive sandstone layer, pertaining to biostratigraphic zones of NP24, was laid down unconformably on the Cretaceous substratum (Huang, 1982). The Oligocene-Miocene stratigraphy of this basin is not well understood due to the homogeneous nature of this thick mudstone which is difficult to correlate using well data. Prior to this study, there was no attempt being made to correlate offshore strata in the above two settings because the drastic lithologic changes to the north and to the south of the Penghu Platform.

North of the Penghu Platform, the Oligocene-Miocene strata are conventionally divided into three cycles of sedimentation, which are

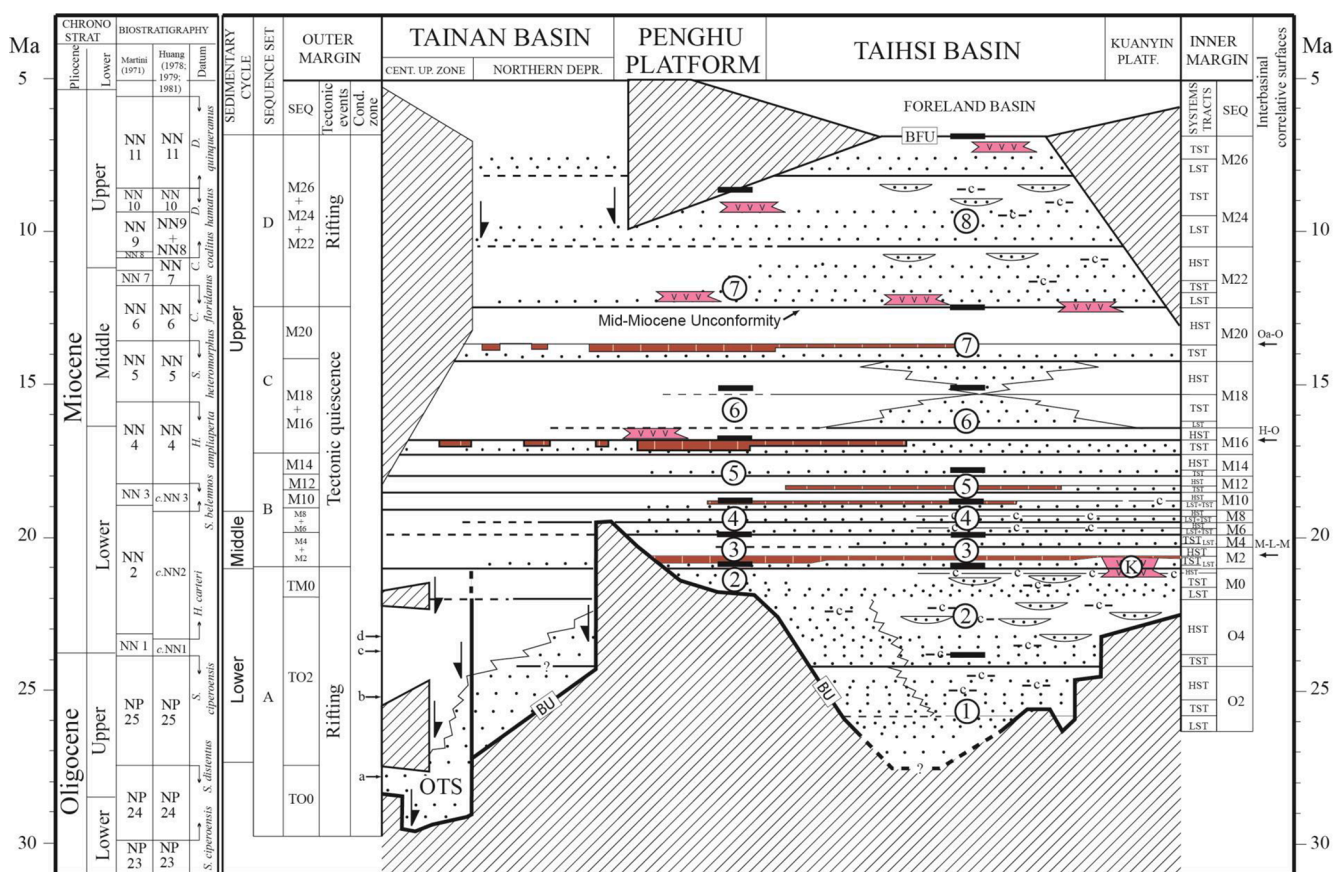


**Fig. 2.** A north to south chronostratigraphy of the Oligocene-Miocene sequences in the west Taiwan basins. The position of this section is roughly as the purple line shown in Fig. 1. Names for newly defined sequences are shown in the left column, and lithostratigraphic units are shown as circled numbers. The three sedimentary cycles are from Chou (1973) and Huang (1982). The horizontal lines with brown color and brick pattern indicate layers of limestones or fossiliferous sandstones. Dots indicate sandstones and areas with oblique lines indicate hiatus. Thick and short horizontal lines indicate formation boundaries. Abbreviations: HST: highstand systems tract, LST: lowstand systems tract, TST: transgressive systems tract; Condensed zones in the Tainan Basin (outer margin) are: a: *S. distentus*, b: *S. ciproensis*, c: *S. delphix*, d: *C. abisectus*. Maximum flooding surfaces in ascending order: M-L-M = *Miogypsina-Lepidocyclina*-Mollusca, H-O = *Heterolepa*-Orbitoid; and Oa-O = *Operculina ammonoides-Operculina*. Lithostratigraphy: 1: Wuchihshan Fm., 2: Mushan Fm., 3: Piling Sh. (or Taliao Fm.), 4: Shihti Fm., 5: Peiliao Fm., 6: Talu Sh., 7: Kuanyinshan Ss., 8 = Nanchuang Fm., K: Kungkuan Tuff, OTS: Oligocene Transgressive Sandstone. (For interpretation of the references to color in this figure legend, the reader is referred to the web version of this article.)

especially evident and well-documented in NW Taiwan (e.g., Chou, 1973; Huang, 1982; Hong and Wang, 1988; Shaw, 1996, Fig. 2). Each cycle is initiated by a step-wise deepening and transgression and ended by a gradual or punctuated shallowing phase. The transgression-regression pairs are represented by three sediment packets, each floored by shallow marine facies and topped by fluvial to paralic deposits with coal measures (Fig. 2).

## 2.1. Three sedimentary cycles

### 2.1.1. Lower Cycle: Oligocene-earliest Miocene (NP24 to mid-NN2)

Sediments of Lower Cycle, pertaining to the biozones of NP24 to middle NN2, were laid down unconformably on Eocene and older strata as drilled in the offshore Taihsi Basin; but the base of Lower Cycle is not exposed in the adjacent northern Western Foothills of Taiwan. This cycle of sedimentation is marked at its base by the paralic to shallow-marine Wuchihshan Formation and the top comprises the coal-bearing, fluvial to coastal facies of the Mushan Formation (Huang, 1982; Yu et al., 1999; Yu et al., 2013; Fig. 2). Near the end of deposition of this sedimentary cycle, mild volcanic activity occurred which also continued into the early stage of the next cycle in NW Taiwan (i.e., the Kungkuan Tuff (K) shown in Fig. 2). This episode of volcanism is coined as Kungkuan stage (Ho, 1988) and dated to occur around 23–20 Ma (Chung et al., 1994; Juang, 1996). In the southern distal margin, thick (~1,000 m) Oligocene-lower Miocene sequence was accumulated in the Tainan Basin. It is represented by a shallow-marine transgressive sandstone (NP24) overlying Mesozoic basement and capped by a marine mudstone layer (NP25-NN1) (Huang, 1982; Lee et al., 1991). Lee et al. (1991) suggested that, based on the foraminiferal paleo-ecological study of the Oligocene sediments, the Oligocene sequence ponded in discrete troughs caused by block faulting. Chen (1993) also reported that, based on sedimentary facies analyses on cores, the Oligocene sediments were accumulated in between NE-SW trending structural highs and depositional lows. Duration for the Lower Cycle is up to ~9 Myr, with oldest sediments being found in the offshore Tainan basin (NP 24).

### 2.1.2. Middle Cycle: Early Miocene (mid-NN2)

In NW Taiwan, the Middle Cycle is initiated by the first regional marine transgression in middle NN2 which laid down the Piling Shale (equivalent to the Taliiao Formation) in a broad shallow sea, which was accompanied by a continued volcanism (Kungkuan Tuff) at its inception (Fig. 2). A coal-bearing coastal facies, the Shihti Formation brought this cycle to an end. The Kungkuan Tuff is succeeded by marine facies with a maximum transgression within zone NN2 to form an isochronous pattern transcending both basins and shelves with the exception of the highest part of the Penghu Platform. The Middle Cycle lasted for about 2 Myr and is the shortest cycle among others.

### 2.1.3. Upper Cycle: Late early Miocene to late Miocene (NN3-NN11)

A renewed marine transgression started in zone NN3 and laid down the shallow-marine Peiliao Formation (Fig. 2). Marine deposition reached a maximum extent during the deposition of the Talu Shale. It was then followed by a marine regression that led to the deposition of the Kuanyinshan Sandstone and concluded with a non-marine to paralic facies of the Nanchuang Formation. During the deposition of the Talu Shale of biozones NN4-NN5 (Huang, 1982), it is considered as the most prominent episodes of transgression for this cycle and during the Oligocene and Miocene epochs. The Upper Cycle is also characterized by an extensive regressive phase accompanying extensive volcanism (the Chiaopanshan stage, Ho, 1988). This episode of volcanism is dated to occur around 13 to 7.1 Ma (Chung et al., 1994; Juang, 1996) and is interpreted to related to intraplate extensions (Chung et al., 1994). The strong regression has resulted in a thick fluvial-paralic sandstone facies, the Nanchuang Formation, overlies shelfal facies separated by a distinctive erosional unconformity, the Mid-Miocene Unconformity shown in Fig. 2, formed during biozones of ~NN6-NN7 (Huang, 1982).

This unconformity is so prominent as to have led some geologists to associate the erosion with the initiation of an orogeny to the east or southeast of Taiwan (Sun, 1982; Tensi et al., 2006). This cycle was brought to an end by orogenic loading that turned the study area into a foreland basin, resulting in an unconformity caused by migrating foreland forebulge (Yu and Chou, 2001, Lin et al., 2003). The Upper Cycle lasts for about 12 Myr.

## 2.2. Marker beds

As pointed out by Huang (1982), the step-wise deepening of the basin occurs usually within a very short stratal interval and is exemplified by a flooding “zone” in the form of a layer of biogenic limestone or calcarenite, which is usually rich in specimens of a single larger foraminiferal species. Six flooding zones in NW Taiwan were reported in Huang (1982) and in Chinese Petroleum Corporation (1985). Three out of the six flooding zones extend to a more distal setting beneath the coastal plain in central Taiwan, where the flooding zones are characterized by the patchy occurrence of limestone beds containing characteristic fauna (e.g., Chi, 1981). These three flooding zones in central Taiwan were named as Mollusca Limestone (early Miocene, NN2), Orbitoid Limestone (Middle Miocene, NN4), and *Operculina* Limestone (Middle Miocene, late NN5), respectively (e.g., Chi, 1981; Chang and Chi, 1983). These flooding zones are labeled as M-L-M, H-O, and OaO in an ascending order as shown in Fig. 2. Since the identification of these flooding zones in both the proximal and distal settings has been made by Chi (1981) and Huang (1982), their potential to serve as inter-basin correlative markers has been overlooked though it was suggested by above authors.

## 2.3. Previous sequence studies

Previous sequence studies focus only on central and northern Taiwan and based largely on outcrop studies. Several authors (e.g., Tai et al., 1994; Tai and Teng, 1994; Yu and Teng, 1995, 1996, 1998; Yu, 1997; Yu et al., 1999; Yu et al., 2013) have reported the Oligocene-Miocene stratigraphic-sequence development in NW Taiwan in the regions of the Hsuehshan Range, Western Foothills and its adjacent offshore basin. They divided the Oligocene-Miocene strata into 19 sequences as concluded mainly from outcrop studies. The above authors suggested that the Oligocene-Miocene sedimentation in northern Taiwan was strongly influenced by eustasy by comparison to the global eustatic curves. This view was also previously endorsed by many other workers (for example, Huang, 1982; Hong and Wang, 1988), though Teng et al. (1991) considered the relative sea-level variations recorded in the Oligocene strata of the Hsuehshan Range essentially to contradict the global sea level fluctuations.

## 3. Data and methods

### 3.1. Data

This study used mainly well logs and biostratigraphic data supplemented by reflection seismic data, covering the areas in the Western Foothills, Coastal Plain and the Taiwan Strait (see Fig. 1 for data coverage). The data sets were provided by CPC Corporation, Taiwan. The well data comprises about 200 boreholes with an average penetration depth of 3,000–3,500 m, including electric wireline logs, lithologic information, biostratigraphy, some velocity check-shot surveys and synthetic seismograms. The wireline logs consist of spontaneous potential and resistivity curves of almost every borehole. Around two-thirds of the boreholes are supplied with gamma ray logs and dozens of logs with sonic velocity, caliper and dipmeter logs. Other reservoir-specific logs, such as porosity logs (e.g., compensated neutron logs, litho-density logs and photoelectric absorption curves) constitute nearly 30 wells but only cover the depth interval of a drill hole with

hydrocarbon-bearing potential. Cutting descriptions from well reports are also used to assist the log facies interpretation wherever available. Index nannofossils for each biostratigraphic zone are extracted from well reports to compile more robust biostratigraphic zonation for the studied sediments.

A total of ~20,000 line-km of multichannel seismic data acquired between 1976 and 1992 were used in this study (Fig. 1). The seismic database consists of a grid of about 5–20 km line spacing. They were used to correlate major sequence boundaries and to map out the sediment isopach, especially in the outer margin (i.e. the Tainan Basin).

### 3.2. Methods on well-log sequence stratigraphy

There are a variety of sequence stratigraphic models in the literature (see Catuneanu, 2017, for a review). We use sequence model proposed by Van Wagoner et al. (1988, 1990) and Christie-Blick (1991) and designated as Depositional Sequence III by Catuneanu (2017) in the present study. The following procedures were observed in constructing the Oligocene-Miocene sequence stratigraphic architecture in the study area.

- (a) Identifications of log facies, log trends, and parasequences at wells: The first step in applying sequence stratigraphy on wireline logs is to interpret individual log facies (Selley, 1995) in terms of depositional parameters, notably the paleo-environments and paleo-water depth. From vertical successions of log facies, flooding surfaces can be recognized such that parasequences (Van Wagoner et al., 1988, 1990) can be delimited. The parasequence is the building block for the well-log sequence stratigraphy. By examining stacking patterns of parasequences, a sequence and its component systems tracts as well as major surfaces may be established (Van Wagoner et al., 1988, 1990, see Section 4).
- (b) Marker Beds: Maximum flooding surfaces were used as primary marker beds for the correlation of the Taiwan Oligocene-Miocene sequences. Several maximum flooding surfaces were recognized in this study. Of these surfaces, three are characterized by the patchy occurrence of relatively thick limestone beds in distal settings, thereby forming the most prominent marker beds in the Taiwan Oligocene-Miocene series (Fig. 2). These three surfaces are named, in this study, after their characteristic fossil species. They are (Fig. 2): (1) *Miogyopsina-Lepidocyclus*-Mollusca of sequence M2 (e.g., M-L-M surface); (2) *Heterolepa*-Orbitoid of sequence M16 (H-O); and (3) *Operculina ammonoides*-*Operculina* of sequence M20 (Oa-O). Of these three maximum flooding surfaces, *Heterolepa*-Orbitoid (M16) is the most extensive marker bed for the studied interval.
- (c) Well correlations: This step involves matching distinctive log patterns among wells and “lining up” the logs at the marker beds. By matching patterns, correlations were made on the basis of log trends on a level of a parasequence or a parasequence set. The well-log sequence stratigraphic correlation was first carried out where closely spaced wells are available in the Taihsi Basin in which the Oligocene-Miocene strata comprise mainly shoreline sequences. The sequence boundaries and stratal surfaces that were recognized in the Taihsi Basin were then correlated to the proximal deposits in the Penghu Basin where fluvial deposits predominated as well as to the distal deposits at the Penghu Platform and the Tainan Basin where shelf facies prevailed.
- (d) Isopach maps for tectono-stratigraphic units: There are 16 sequences recognized in the Oligocene-Miocene strata and they are grouped into four sequence sets (i.e., sequence sets A, B, C, and D). To the north of the Penghu Platform, isopach maps for these four sequence sets were prepared using thickness data at wells or outcrops wherever possible. To the south of the Penghu Platform and in the Tainan Basin, sediment thickness was based on

borehole data as well as results from seismic interpretation because of the poor borehole coverage there.

## 4. Identifications of parasequences, key surfaces and sequences

### 4.1. Parasequences, flooding surfaces, and parasequence sets

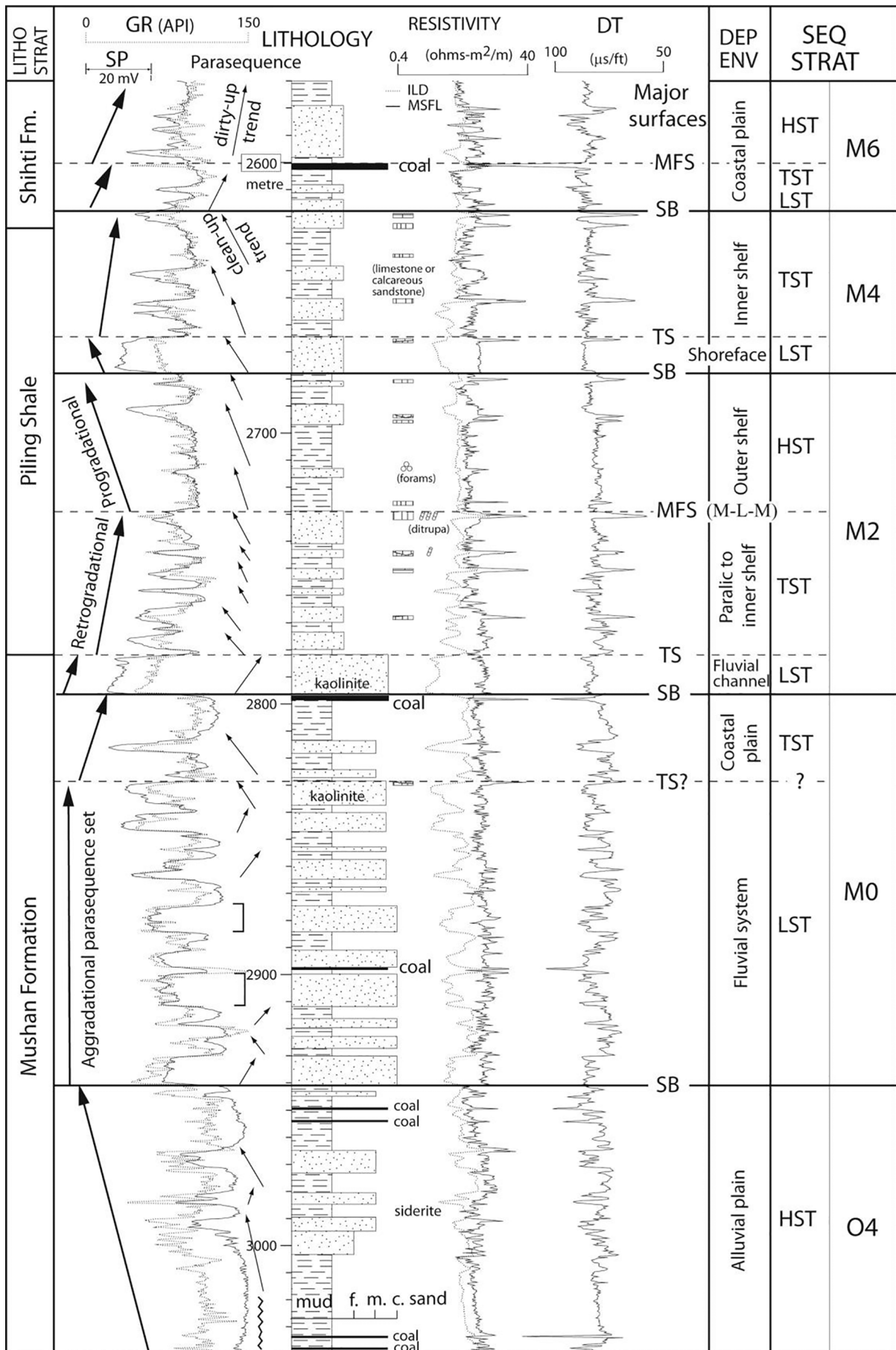
A number of distinctive log trends for individual parasequences expressed in terms of gamma-ray logs are recognized in the studied Oligocene-Miocene records (e.g., Fig. 3). The shapes of gamma-ray curves resemble grain size successions (e.g., Selley, 1995). We also incorporate other environmentally “diagnostic” information (from cuttings or cores, for examples) wherever possible, such as the presence and abundance of coal beds, carbonaceous matter, marine fossils, and diagnostic minerals (e.g., glauconite and kaolinite) to assist environmental interpretation for each log trend. Using well BK16 for example (Fig. 3), main recognized trends for the Taiwan Oligocene-Miocene series include the following: (a) Cleaning-up trend: The cleaning-up motif may represent a prograding, sandy shoreline succession, a depositional unit at a shallow-marine setting that shows an upward increase in depositional energy, a crevasse splay building into an inter-distributary bay etc. (b) Dirtying-up trend: This trend may be the product of a fluvial point-bar succession, tidal channel/estuarine point-bar deposits, a mud-dominated and prograding tidal shoreline, the retreat or abandonment of a shoreline-shelf system, etc. (c) Boxcar trend: Boxcar log-trends are typical of some types of fluvial channel sands (amalgamated channel sands, for example) in the study area. The above cyclic-log trends may be identified as parasequences bounded by flooding surfaces; other log trends, however, are difficult to recognize as individual parasequences. One example is the irregular trend as shown in Fig. 3. It has no systematic change in either base line, and it lacks the clean character of the boxcar trend. It represents the aggradation of a shaly or silty lithology, and may be typical of alluvial plain as the case for well BK16 (Fig. 3) or more typically, shelfal or deep-water settings, as commonly found in wells from the Miocene sediments of the Tainan basin.

Parasequences are bounded by flooding surfaces (Van Wagoner et al., 1988, 1990). The studied sediments are of fluvial to shallow marine origin. It is therefore desirable to correlate flooding surfaces from a marine realm to non-marine settings. In doing so, in marine settings, this surface is commonly recognized as an abrupt upwards increase in shale content. It may also coincide with a thin transgressive lag horizon expressed usually as a thin bed consisting of fossiliferous and coarser-grained sediments. In coastal plain settings, a major dislocation in the depositional environment and a landward shift in facies may mark the flooding surface as suggested by Kamola and Van Wagoner (1995). Flooding surfaces (i.e. parasequence boundaries) may, however, become obscure in fluvial and coastal plain settings because of the lack of the facies contrast necessary to make flooding surfaces visible. We used lateral extensive and thick coals, coastal-plain mudstones as suggested by Van Wagoner (1995) as updip correlative marine-flooding surfaces in non-marine settings.

A parasequence set is a succession of genetically related parasequences that form a distinctive stacking pattern bounded by major flooding surfaces and their correlative surfaces (van Wagoner et al., 1990). The types of vertical arrangement (stacking patterns) of parasequences are the results from the competing effects of rates of accommodation space generation (or destruction) and sediment supply. There are three types of stacking patterns seen in our studied well logs as shown in Fig. 3, for examples: progradational, aggradational, and retrogradational stacking patterns, respectively.

### 4.2. Identifications of key surfaces, systems tracts, and sequences

Key surfaces here refer to sequence boundaries, transgressive surfaces, and maximum flooding surfaces. In this section, we discuss the identifications of sequence boundary, lowstand systems tract,



(caption on next page)

**Fig. 3.** An example well (BK16 well in the Taihsi Basin) showing how lithology, log trends, depositional environments, sequences and their component systems tracts are defined using well-log patterns. Four types of log trends are found with different symbols: cleaning-up trend (upper left pointing arrow), dirtying-up trend (upper right pointing arrow), box-car trend (vertical line with sticks at both ends), and irregular trend (wiggly line). Log curves: DT: sonic interval transit time, GR: gamma ray, ILD: dual induction-laterolog (measuring deep resistivity), MSFL: micro-spherically focused log (measuring shallow resistivity), SP: spontaneous potential; major surfaces: MFS: maximum flooding surface, SB: sequence boundary, TS: transgressive surface.

transgressive surface, transgressive systems tract, and highstand systems tract.

4.2.1. Sequence boundary

The criteria (Van Wagoner et al., 1990) that identify the unconformable part of sequence boundaries include a basinward shift in facies. That is an abrupt shift to shallow facies above the unconformity as well as a vertical change in parasequence stacking pattern and log facies. For examples, the lower boundary of sequence M2 (Fig. 3) is marked by an erosional surface underlain a laterally extensive fluvial sandstone resting on coastal plain fines. Downdip, in a shelf setting, a basinward shift in facies may juxtapose fluvial strata on marine shales, such as the

case of the lower sequence boundaries of M6 (Fig. 3). Farther downdip, the basinward shift of facies may be manifested by a sharp-based shoreface sandstone overlying offshore muds forming a truncated cleaning-up log trend as exemplified at the lower M4 sequence boundary (Fig. 3). This abrupt shift is called a forced regression by some workers (e.g., Posamentier et al., 1992); also, sediments deposited during the time when relative sea level is falling are also coined falling stage systems tract by some worker (Plint and Nummedal, 2000). The boundary is interpreted as regressive surface of marine erosion but not sequence boundary (e.g., Plint, 1988). Farther downdip, in a basinal setting, like in the distal margin (e.g., the Tainan basin) the correlative conformity may display no obvious facies contrast or other unusual features; the

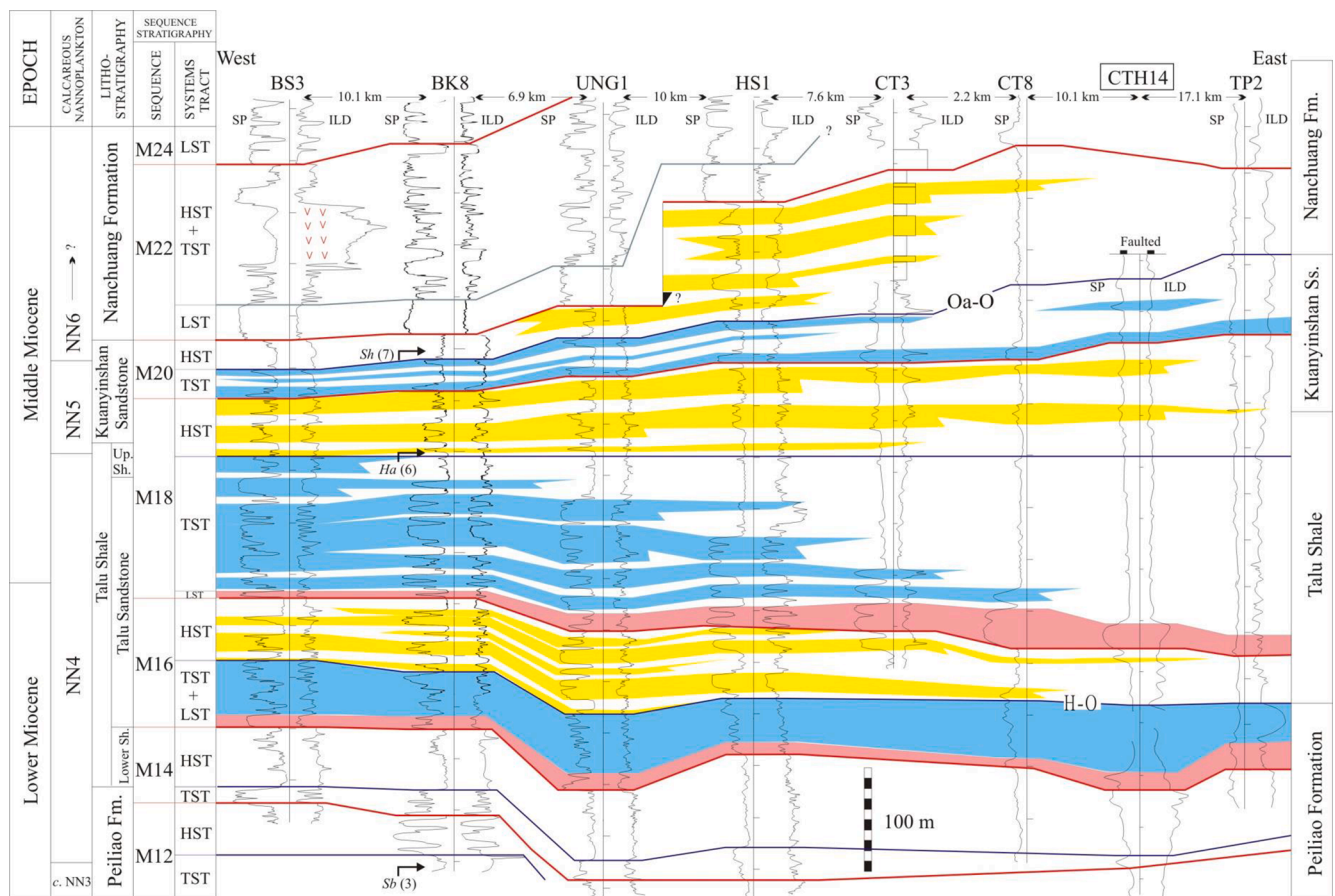


**Fig. 4.** A dip-oriented well-correlation panel in the Taihsi Basin showing the parasequence stacking patterns of the sequence set C (see Fig. 11 for well locations and Fig. 12 for a correlation panel of the same stratigraphic interval oriented obliquely across the South China margin). Sequence M18 shows particularly well the definition of systems tracts in terms of parasequence stacking pattern. The lower M18 sequence boundary is defined by a basinward shift in facies (at CTH14, for example). The strong regression led to the development of a layer of tens-of-meters thick sandstone (i.e., a lowstand systems tract, LST), overlying sharply on the offshore mudstone. The ensuing marine transgression led to a strong retrogradational (back stepping) stacking pattern which forms the transgressive systems tract (TST) and records the westward marine transgression. The switch from retrogradational to progradational (highstand systems tract, HST) parasequence stacking pattern marks the maximum flooding surface (MFS). The LST of M18 is equivalent to the “Chinshui Zone 13” Sandstone of Huang (1976) in a basinal setting. The last occurrences for the zonal marker nannofossils are shown alongside the BK8 well (e.g., Ha) together with the number (in brackets) of wells that show a similar stratigraphic level for the last occurrence of the following index nannofossils: Ha: *H. ampliaperta*, Sb: *S. belemnos*, and Sh: *S. heteromorphus*. The abrupt increase of the M20 thickness between wells UNG1 and HS1 indicates that a phase of normal faulting may have initiated during the deposition of the upper M20 sequence and continued into the late Miocene (see Fig. 12 of Lin et al. (2003) for the inferred normal faults that were active during the late Miocene). Abbreviations can be found in Fig. 2.

position of the sequence boundary in this case can only be approximated. The sequence boundary in thick fluvial successions is difficult to identify, but it may be best identified from the stratal geometries that signify an abrupt change in the rate at which accommodation space was created (Shanley and McCabe, 1994). In our studied thick fluvial sequences (usually a few hundred meters thick), the sequence boundary is placed at where a sudden vertical increase in channel stacking and amalgamation pattern (i.e., abrupt changes in alluvial architecture) such as the lower sequence boundary of M0 shown in Fig. 3.

#### 4.2.2. Lowstand Systems Tract (LST, Fig. 3)

The lowstand systems tract is the set of depositional systems active during the time of relatively low sea level following the formation of the sequence boundary. At a ramp-type setting (i.e., without a distinct shelf-slope break, such as the west Taiwan basins during the Oligocene-Miocene time), the lowstand systems tract typically consists of narrow to broad incised valleys, usually filled with tide-dominated deltaic deposits and age-equivalent, updip fluvial strata (Van Wagoner et al., 1990). In a nonmarine realm, braided fluvial systems and amalgamated channel infills are most likely to occur in the lowstand systems tract and rest on the sequence boundary (e.g., Kerr et al., 1999; Leckie et al., 2004; Shanley and McCabe, 1993; Van Wagoner, 1995). The lowstand systems tract defined here includes the falling stage systems tract of Plint and Nummedal (2000).

#### 4.2.3. Transgressive Surface (TS, Fig. 3)

The lowstand and transgressive systems tracts are separated by the transgressive surface above which flooding occurs. The transgressive surface represents the first major flooding surface to follow the sequence boundary and is usually distinct from the relatively minor flooding surfaces that separate parasequences in the lowstand systems tract. In updip areas characterized by subaerial exposure and erosion during the deposition of the lowstand systems tract, the transgressive surface and sequence boundary are merged into a single surface.

#### Transgressive Systems Tract (TST, Figs. 3, 4)

The transgressive systems tract consists of a retrogradational set of parasequences, the TSTs of M2 (Fig. 3) and M18 (Fig. 4) being the prime examples in this respect. It is underlain by the transgressive surface and overlain by the maximum flooding surface. As in any retrogradational set of parasequences, flooding surfaces within the transgressive systems tract are unusually prominent and display strong facies contrasts and pronounced deepening. Because the parasequences back-step, the transgressive systems tract displays an overall deepening-upward succession, although each component parasequence is shallowing-upward.

#### 4.2.4. Maximum Flooding Surface (MFS, Fig. 3)

The transgressive and highstand systems tracts are separated by the maximum flooding surface which represents the most landward position of the shoreline. This occurs when the provision of new space for topset accumulations has slowed to a point where it is matched by sediment supply, and it marks a switch from retrogradational to progradational parasequence stacking pattern. The maximum flooding surface, especially in a basinward position, is starved of coarse clastics for a considerable period of time and is usually marked by a condensed section. Condensation or slow net deposition allows more time for diagenetic reactions to proceed and more skeletal material to accumulate. The maximum flooding surface is therefore usually recognized, in the Taiwan region, as marked by fossiliferous horizons or shell beds in basinward positions. For example, the maximum flooding surfaces of *Miogypsina-Lepidocyclus*-Mollusca (M2), *Heterolepa*-Orbitoid (M16), and *Operculina ammonioides-Operculina* (M20) in the Taiwan region are shown in Fig. 2 as M-L-M, H-O, and Oa-O, respectively.

In some nonmarine units, surfaces similar to condensed sections may be characterized by thin extensive coals, thin brackish to marine shales and lacustrine limestone. Also, invasion of tidal processes into areas formerly dominated by purely fluvial process is the temporal equivalent

of a maximum flooding surface (Shanley and McCabe, 1994). In the Taiwan region, thin extensive coals have been found in M0 (top Mushan Formation, Fig. 3), M6 and M8 (Shihti Formation) that are interpreted as equivalent maximum flooding surfaces in a nearshore nonmarine setting.

#### 4.2.5. Highstand Systems Tract (HST, Fig. 3)

The highstand systems tract consists of an aggradational to progradational set of parasequences that overlies the maximum flooding surface and that is overlain by the next sequence boundary. As the parasequences pass from aggradational to progradational stacking, the flooding surfaces are increasingly subdued at the expense of overall shallowing. The highstand systems tract in a nonmarine setting may be characterized by flood plain fines with isolated point bar sandstones (e.g., Shanley and McCabe, 1993; Van Wagoner, 1995).

Finally, it is important to stress that not all of these surfaces or systems tracts may be present within any given sequence. For example, lowstand systems tracts are commonly absent in updip areas where the transgressive surface and sequence boundary are merged as one surface. In such areas, the sequence boundary is marked by the beginning of retrogradational stacking.

From the above practice we have been able to identify 16 sequences and related key surfaces and correlate them among basins in the study area. The 16 Oligocene-Miocene sequences are named alpha-numerically and using an even numbering scheme from older to younger sequences. The even numbering scheme has the flexibility for additional sequences to be inserted (e.g., M3) if identified in subsequent works. The letter O represents Oligocene and M denotes Miocene. In addition, the age assignment (i.e., O or M) for individual sequences is based on the age of its lower sequence boundary. All post-breakup sequences can be correlated inter-basinally, except for the Oligocene sequences in the Tainan Basin. Therefore, the Tainan Oligocene sequences are named TO0 and TO2 (with T representing the Tainan Basin), while Oligocene sequences in other basins are named O2 and O4. For the Miocene succession, there are 13 sequences (M2 to M26) that can be correlated inter-basinally.

## 5. Biostratigraphic framework

The new biostratigraphic framework (left columns in Fig. 2) presented in this work is compiled from well reports, and is calibrated by stratal surfaces correlated among wells carried out in the present study. It has also been supplemented wherever possible by existing publications and unpublished biostratigraphic charts. Moreover, a few K-Ar ages from the early and late Miocene basalts, in particular those ages reported in Juang (1996), serve as additional age constraints. The biostratigraphic zonation reported in well-completion reports were carried out by examining samples from well cuttings, sidewall cores, and continuous cores. Cuttings were usually sampled for every five or ten meters, however, the taxa contained therein were possibly contaminated by downhole caving and reworking due to drilling activities. It renders the identification of the first occurrences (FO) of a specific bio-event less easy and ambiguous. Only stratigraphic last occurrences (LO or "tops") can be obtained for biostratigraphic correlations using cutting samples. In contrast, samples from continuous or sidewall cores are usually free from contamination by downhole cavings. Because the sidewall cores were usually sampled every tens of meters, they were used extensively in establishing the biostratigraphic framework reported in the well-completion reports. The first occurrences (FO) of bio-events can therefore be confidently identified using core samples rather than by examining cuttings.

The present sequence stratigraphic correlation, carried out on a grid of closely spaced wells has found that the reported individual bio-horizons (i.e., FO or LO) at wells scatter vertically (up to hundreds of meters, for example) about lateral persistent stratal surfaces. Since the stratal surfaces found at closely-spaced wells are depositional surfaces,

they are essentially time-synchronous. The stratal surfaces correlated between wells were therefore used to refine the biostratigraphic framework in this study. One example of fine tuning a zonal boundary on the basis of the stratal surface correlation comes from the NN4/NN5 boundary (e.g., Fig. 4). This zonal boundary is based on the last occurrence of the *Helicosphaera ampliaperta* (labeled as Ha) alongside the BK8 well in Fig. 4). This boundary has been traditionally placed (e.g., Huang, 1976; Yu, 1997) on top of the “Chinshui Zone 13” sandstone at a down-dip outcrop section (i.e., the Chuhuangkeng section) in northern Taiwan; also the “Chinshui Zone 13” sandstone of (Huang, 1976) is equivalent to the lowstand systems tract of M18 according to the sequence framework presented in this work. On the basis of sidewall core data, there are six wells which show that the last occurrence of *Helicosphaera ampliaperta* occurred slightly above the maximum flooding surface of M18. It is therefore evident that the NN4/NN5 boundary should be placed near the M18 maximum flooding surface instead of the previous assignment of Huang (1976). One should note that a partial reason for Huang’s assignment of NN4/NN5 boundary on top of the “Chinshui Zone 13” sandstone was because the strata of ~130 m thick that immediately overlies the assigned NN4/NN5 boundary were not sampled by him.

Only nannofossil bio-events were used in this study because the majority of bio-horizons reported in the well reports are nannofossil datum planes. Thirteen nannofossil datum (Fig. 2) were used in this study ranging from late Oligocene to Miocene (NP24-NN11) as reported in Huang (1976, 1978, 1982). The nannofossil zonal scheme of Taiwan, from NP24 to NN11, is similar to the worldwide standard of Martini (1971) except that the definitions of zones NN1, NN2, and NN3 are slightly different from that of Martini (1971). For this reason, the equivalent Taiwan NN1, NN2 and, NN3 zones are written c.NN1, c.NN2, and c.NN3 for simplicity. The ages for the zonal boundaries are according to Berggren et al. (1995).

The stratal surfaces correlated among wells and additional age constraints from basalts (Juang, 1996) have led not only to a significant improvement on the consistency among wells of the Oligocene-Miocene biostratigraphy, but also to a modification of the dating of three rock formations of the Mushan Formation, Piling Shale and the Nanchuang Formation. These refined ages presented in this study also provide improved timing for major stratal surfaces and tectonic events.

The lower Miocene, nonmarine Mushan Formation (labeled as 2 in Fig. 2) is barren of age-diagnostic fossils. It was previously thought to fall within c.NN1 (e.g., Huang, 1978) because it overlies the Wuchihshan Formation (labeled as 1) which contains NP25 fossils (Huang, 1979a) and underlies Piling Shale (labeled as 3) which contains c.NN2 fossils. According to this biostratigraphic scheme, the age for the upper Mushan Formation and basal Piling Shale would be around 23 Ma (i.e., upper c.NN1 to lower c.NN2) according to the chrono- and biostratigraphic schemes of Berggren et al. (1995) (Fig. 2). The K-Ar dates from basalts i.e., the Kungkuang Tuff (labeled as K), that are hosted near the base of the Piling Shale in onshore NW Taiwan (Juang, 1996) yielded three ages, 20.0+/-0.5 Ma, 19.9+/-0.5, and 19.1+/-0.4 Ma. All the basalt age dates (i.e., from 19.1 to 21.2 Ma) are consistent in terms of their stratigraphic levels but are all younger than the previously perceived age (i.e., ~23 Ma) for the host formations. It should be noted that the age from K-Ar dating may show a younger age of up to 10% of the dated age based on a comparison of astronomical ages and results from the new  $^{40}\text{Ar}/^{39}\text{Ar}$  dating method (Renne et al., 1994; Hilgen et al., 1999).

The age for the Mushan Formation/Piling Shale boundary, which corresponds approximately to the lower M2 sequence boundary, can be estimated at ~21 Ma on the basis of these new age dates. This age is in middle c.NN2 which implies that the Piling Shale belongs to upper c.NN2 instead of lower c.NN2 as previously conceived. In addition, the co-occurrence of c.NN2 and N5 zonal marker fossils (e.g., Huang, 1980; Huang and Cheng, 1983) in the Piling Shale further supports the dating of the Piling Shale as the upper c.NN2 according to the biostratigraphic

scheme of Berggren et al. (1995). The c.NN1/c.NN2 boundary (23.2 Ma) may also be estimated by linear interpolation between the upper age, 21 Ma, at the top Mushan Formation and the lower age, 23.9 Ma, top NP25, which corresponds approximately to the base of the Mushan Formation. This practice places the c.NN1/c.NN2 boundary in the lower Mushan Formation (Fig. 2), indicating that much of the Mushan Formation is in c.NN2 rather than in c.NN1 as previously suggested.

The upper Miocene, mostly nonmarine Nanchuang Formation (labeled as 8) has been difficult to date. The dating for this formation, however, is indicated by its underlying Kuanyinshan Sandstone (labeled as 7), pertaining to NN6 biozone, and overlying NN11 Kueichulin Formation (Huang, 1976). The Nanchuang Formation was thus tentatively regarded to fall in NN 7 (or NN6?) to NN10 (or NN11?) (Huang, 1976; Huang, 1979b) which correspond approximately to the interval 13.6 to 8.6 Ma. The lower part of this tentative biostratigraphic scheme is also supported by a marker nannofossil species (Huang, 1979b), *Catinaster coalitus*, indicative of NN8 or lower NN9 identified in the lower Nanchuang Formation in central Taiwan.

The present study suggests that the Nanchuang Formation most likely spans the interval mid-NN6 to mid-NN11 which corresponds to the range around 12.5 to 6.5 Ma. The assigned age for the top Nanchuang Formation (i.e., 6.5 Ma, middle NN11) is on the basis of new basalt age dates (Juang, 1996) as well as an NN11 marker fossil, *Discoaster quinqueramus*, which was identified in the upper Nanchuang Formation, and this has been discussed in Lin et al. (2003). The assigned lower age (middle NN6) is based on the fact that the Nanchuang Formation overlies NN6 sediments of the Kuanyinshan Sandstone (Fig. 4). This may indicate that the boundary of the Kuanyinshan Sandstone/Nanchuang Formation (mid-Miocene unconformity, see discussion in Section 6.3) may still be in zone NN6. Therefore, the age of the above boundary has been determined to be around 12.5 Ma, an averaged age for NN6 sediments (Fig. 2).

## 6. Sequences

### 6.1. Sequence Set A: Oligocene to Early Miocene (~30–21 Ma)

Sequence set A is bounded by the breakup unconformity below (Lin et al., 2003) and the upper M0 sequence boundary above (or the lower M2 sequence boundary, Figs. 2, 5). The strata that directly overlies the breakup unconformity show an overall younger age towards the inner continental margin and span the biozones of NP24 in the outer margin (i.e., the Tainan Basin) to c.NN2 in the inner margin (e.g., the Penghu Basin). The upper boundary, however, is in middle c.NN2 and is dated 21 Ma as described in the preceding section.

Sequence set A (Figs. 2, 5, 6, 7) represents the early post-breakup phase (~30–21 Ma) of basin-infilling and accumulated in two depocenters, to the north and to the south of the NE-SW trending Penghu Platform. In the northern depocenter a sand-prone fluvial to paralic succession (NP25 to lower c.NN2) unconformably overlies the Eocene syn-rift sediments in the west. In the southern depocenter (i.e. Tainan Basin), a thick, fault-bounded marine unit (NP24 to lower c.NN2) was ponded to the south of the Penghu Platform on top of the Mesozoic basement. The lithofacies and sequence development in the north and south depocenters are very different owing to their differences in basin subsidence mechanisms (i.e., thermal vs. fault-controlled subsidence in the north and south respectively, Lin et al., 2003) together with the presence of an emergent rift shoulder, the Penghu Platform, in between. The rift shoulder effectively trapped coarse sediments that sourced from China in the northern depocenter leading to the deposition of mostly marine fines in the Tainan rift basin in the south.

The equivalent lithostratigraphic units and sequences are the followings (Figs. 2 and 7): (1) Taihsi Basin - the Wuchihshan Formation is equivalent to sequence O2 and lower O4 sequence, and the Mushan Formation is equivalent to upper O4 sequence and sequence M0; and (2) Tainan Basin - “Oligocene Transgressive Sandstone” (TOO) and the shale

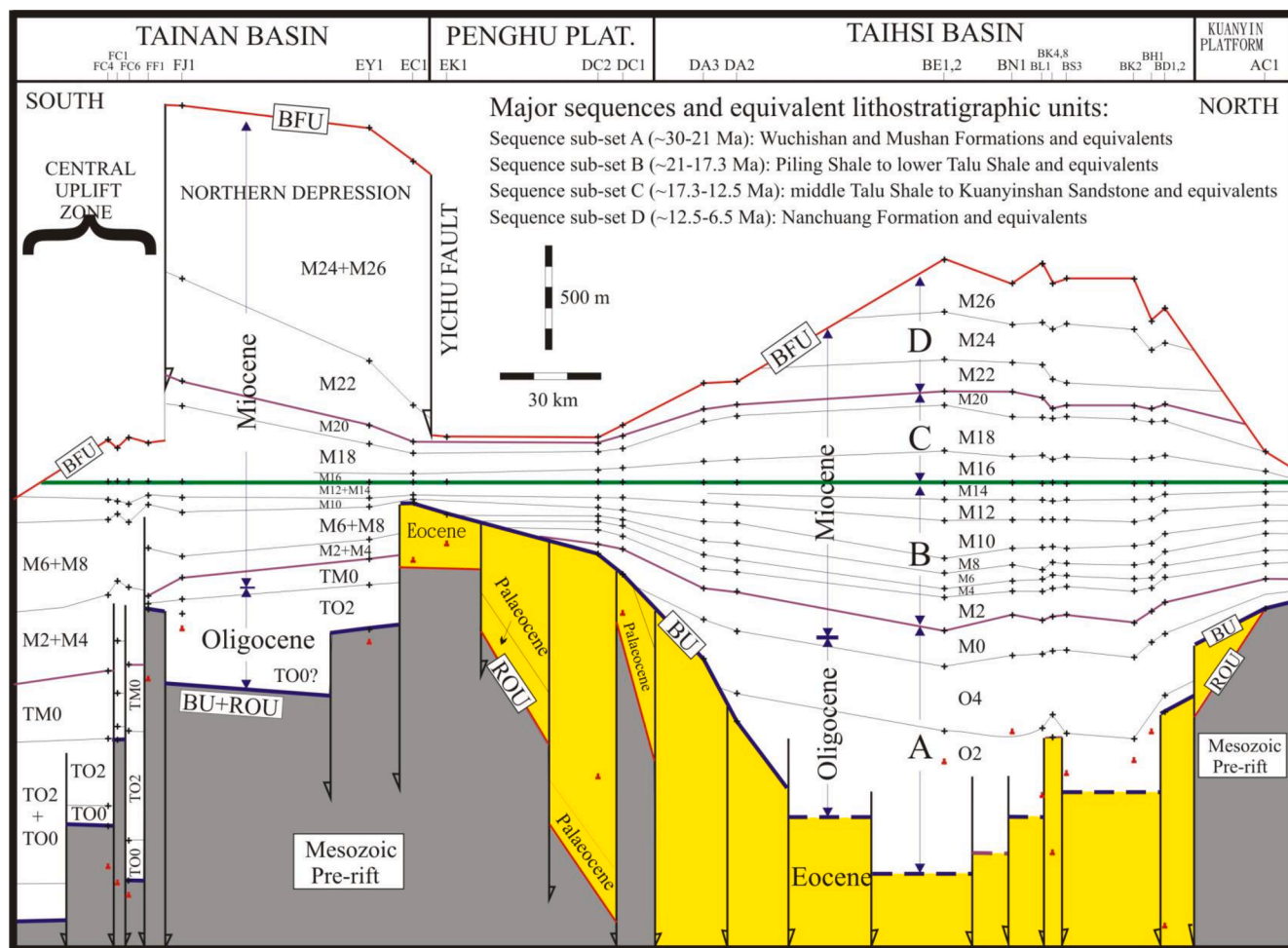


**Fig. 5.** North to south variability in the sedimentary thickness of the Oligocene-Miocene passive margin sequences across the Taiwan margin (see Fig. 1 for well locations). The post-breakup sequence is divided into 16 unconformity-bounded sequences (O2 to M26 which can be grouped into A, B, C, and D four sequence sets). Note the local fault-bounded troughs in the Tainan Basin and adjacent erosional hiatuses during the sedimentation of sequence sets A and D. Sequence sets B and C have evenly blanketed the studied region. The datum plane (thick horizontal line) is the sequence boundary of sequence M16 (middle Miocene). Lower sequence boundary of M22 denotes the mid-Miocene unconformity. Unconformities of rift-onset unconformity (ROU), breakup unconformity (BU) and basal foreland unconformity (BFU) are from Lin et al. (2003).

bed of NP25 to lower c.NN2 (TO2 and TM0). Because the rock formations in the Tainan and Penghu Basins have not been formally defined in the literature, the equivalent lithostratigraphic units and sequences in these two basins are therefore not given in this work. Stratigraphic and biostratigraphic data suggest diachronous sequence development in the north and southern depocenters. Therefore, the stratigraphic sequences in these two depocenters are described separately.

#### 6.1.1. Sequence Set A in the Northern Depozone (Taihsi Basin)

The sand-prone fluvial to paralic succession (NP25 to lower c.NN2) in the west thickens and grades basinward to a marine unit in the Hsuehshan Range where continuous NP23 to lower c.NN2 sedimentation is evident (Huang, 1978; Teng et al., 1991; Yu et al., 2013). Because the Hsuehshan Range is not covered by the subsurface dataset used in this study, we shall limit our discussion to the west Taiwan basins where subsurface data are available. Interested readers may refer to Yu et al. (2013) where the correlation of outcrop sections and subsurface well logs in the Northern Depozone is discussed. Nevertheless, the equivalent thickness in the Hsuehshan Range for the sequence set A (formations Szeleng Sandstone to Aoti Formation shown in Fig. 4 of Lin et al., 2003) and that in the Western Foothills (e.g., the Wuchihshan and Mushan Formations, Teng et al., 1991; Yu

et al., 1999, Yu et al., 2013) were incorporated to construct the isopach of the sequence set A shown in Fig. 6.

Following a period of erosion accompanied by the development of the Oligocene breakup unconformity, a marine transgression firstly inundated the former rift center during NP25 in the Taihsi Basin. This led to the deposition of a sand-prone sequence (O2, Fig. 7) of shallow marine to coastal plain origin that was restricted to the former rift depocenter. An ensuing relative sea-level drop in late NP25 brought the environment into a nonmarine regime and laid down the nonmarine upper Wuchihshan and Mushan Formations. During the deposition of the above formations, the basin grew wider and wider and resulted in the progressive onlapping of younger sediments onto the neighboring basement highs (Fig. 5).

The main feature for the nonmarine succession (e.g., the upper Wuchihshan and Mushan Formations, labeled as 1 and 2, respectively in Fig. 7) is the cyclic development of a laterally extensive and thick fluvial channel sandstone layer that grades vertically into fine-grained sediments containing isolated sand bodies and coal beds (see Figs. 3, 7, for examples). The sequence boundary in this succession is therefore recognized as a surface that separates thick mudstone below from the laterally extensive, fluvial channel sandstones above. The nonmarine succession was accordingly divided into sequences O4 and M0. Although

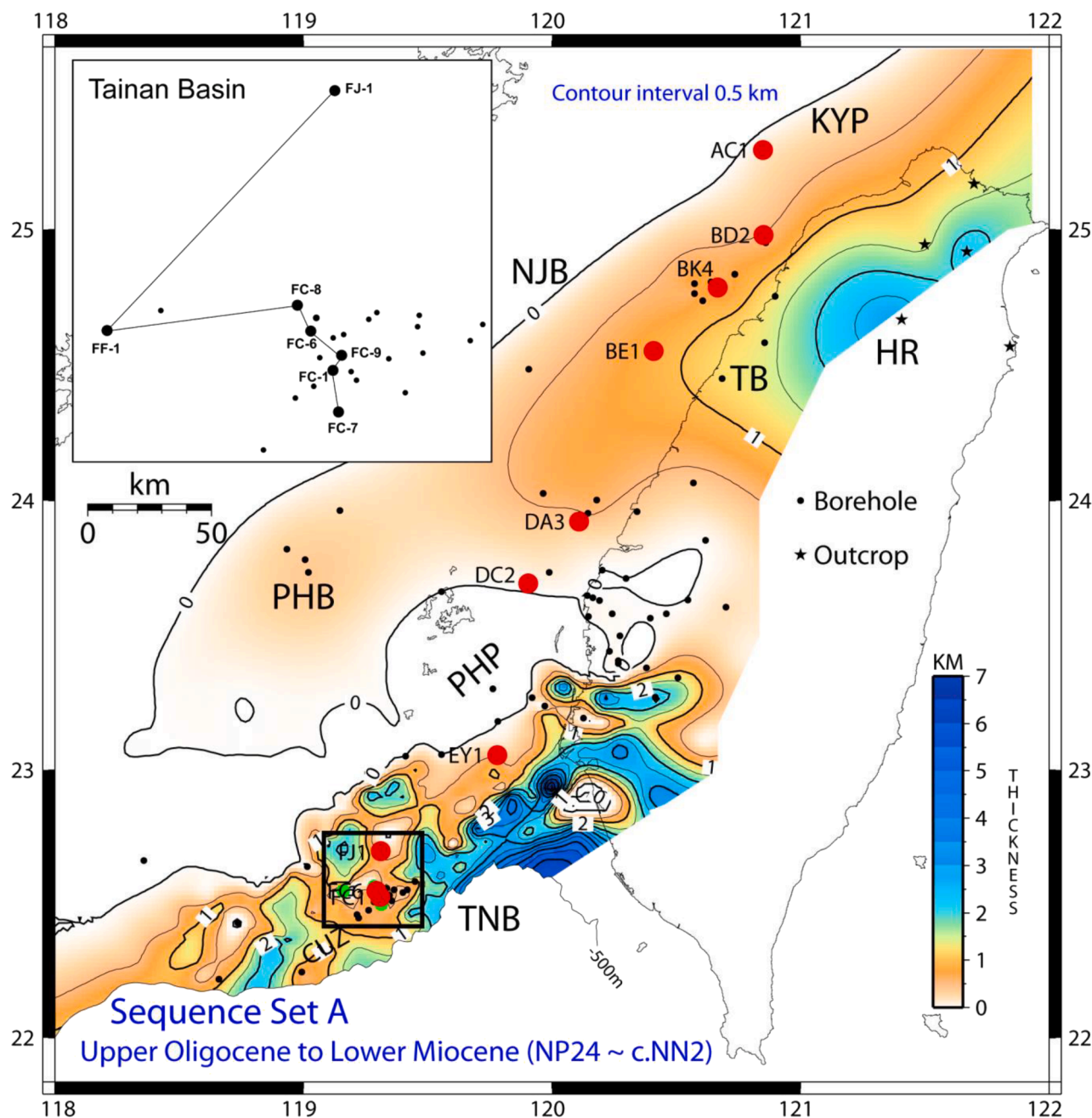


**Fig. 6.** Sediment isopach of the sequence set A (Lin et al., 2003). In the northern depocenter, including tectonic elements of HR (Hsuehshan Range), KYP (Kuanyin Platform), NJB (Nanjihntao Basin), PHB (Penghu Basin), and TB (Taihsi Basin), the thickness data for the sequence set A were mainly drawn from boreholes (dots) and outcrops (stars), whereas in the PHP (Penghu Platform) and TNB (Tainan Basin), additional control points from seismic data were used. Red dots show the borehole locations for the north-south well-log correlation panel shown in Fig. 7. The sequence architecture in the Tainan Basin is also shown in Fig. 8 at wells connected by a green line as shown in the inset figure. CUZ: Central Uplift Zone, (For interpretation of the references to color in this figure legend, the reader is referred to the web version of this article.)

the recognition of the sequence boundary in the nonmarine succession appears to be relatively unambiguous, the identification of the transgressive surfaces is problematic. Also, in the lack of a laterally extensive coal bed, the identification of maximum flooding surfaces in the nonmarine succession is also ambiguous, for example, sequence O4. For these reasons, the subdivision of a nonmarine sequence into its component systems tracts was not attempted in this study if a laterally extensive coal bed is absent in the nonmarine succession.

A few marine agglutinated forams were found at downdip wells (e.g., at the BK1, CT1, and TCS1 wells) at a stratigraphic level that is similar to the nonmarine fines of upper M0 at updip wells. The marine forams at

downdip locations suggest a marine invasion occurred at the close of M0 deposition. This line of evidence links the nonmarine fining-upward trend, in particular sequence M0, to an increase in water depth. Furthermore, at a similar stratigraphic level (top M0), a thin (less than 3 m thick) and persistent coal bed (Figs. 3, 7) can be correlated downdip in a distance of ~50 km in the northern Taihsi Basin. An extensive coal seam is commonly used as an indicator of base-level rise (e.g., Cross, 1988; Aitken and Flint, 1995) and this interpretation is in accord with the existence of coeval marine forams at downdip locations noted above. The transgression near the end of the M0 deposition also inundated the eastern part of the previously emergent rift shoulder (the Penghu

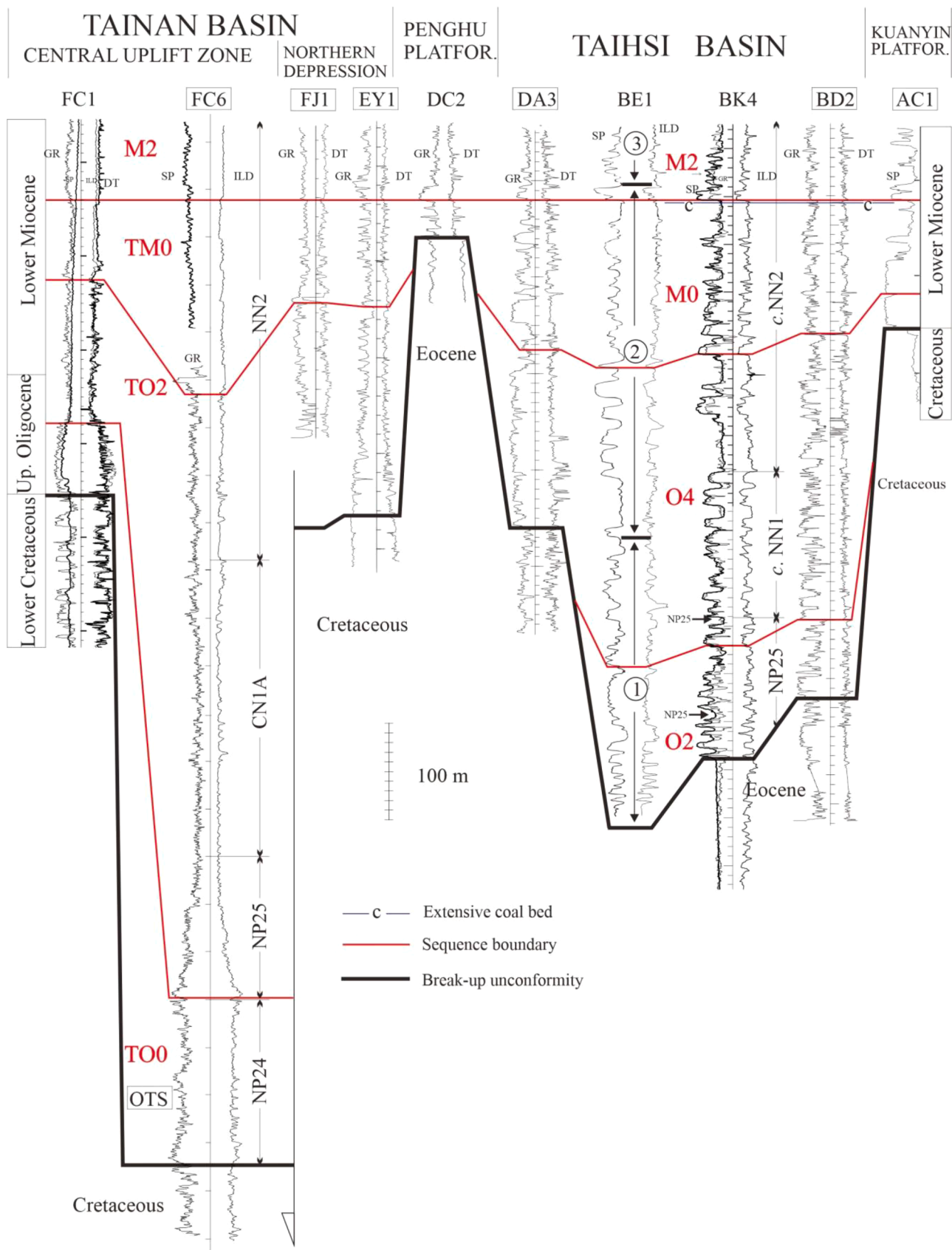


Fig. 7. Sequence variability from inner margin (right) to outer margin for the sequence set A (see Fig. 6 for well locations). Rock formations are numbered as those in Fig. 2. OTS: “Oligocene Transgressive Sandstone”. Arrows alongside the BK4 well indicate the stratigraphic level where NP25 index fossils were identified from sidewall core samples at the BK4 well or at nearby wells. Each well name outlined by a square is a well where the amount of tectonic subsidence is illustrated in Fig. 14 of Lin et al. (2003); this also applies to all the well-correlation panels in the following figures presented in this paper.

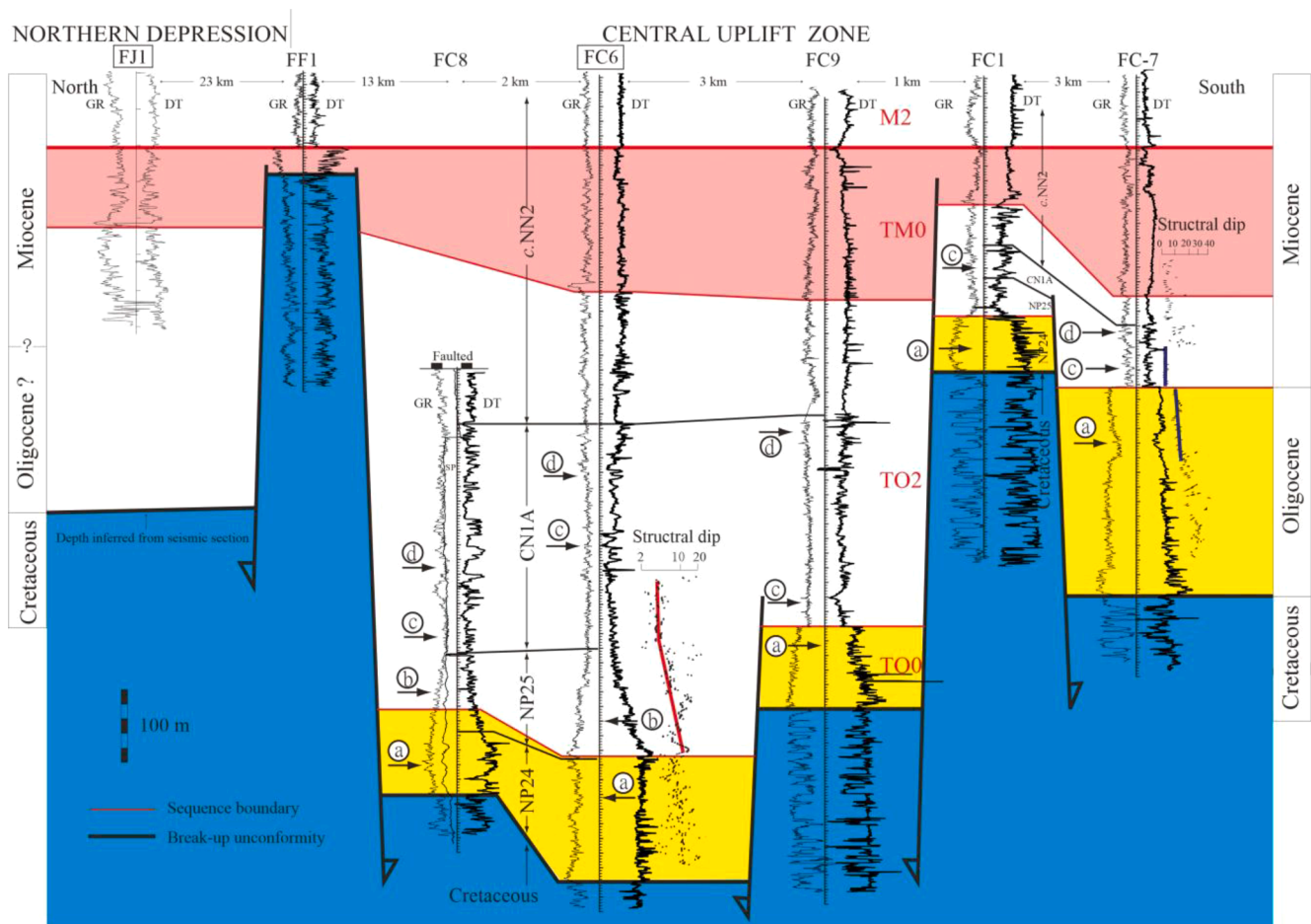


Fig. 8. Sequence correlation for the sequence set A in the Tainan Basin (for well locations see the inset figure in Fig. 6). The three sequences, TO0, TO2, and TM0, are color coded as yellow, white, and pink respectively. The letters, a, b, c, and d, are nanofossil acme zones explained in Fig. 2. (For interpretation of the references to color in this figure legend, the reader is referred to the web version of this article.)

Platform) on central-western Taiwan; while the main part of the rift shoulder remained emergent (Fig. 6).

The fluvial systems in the north graded into coarser-grained and thick shoreline deposits in the south, bordering the Penghu Platform (the DA3 well shown in Fig. 7, for instance). This thick shoreline succession shows overall aggradational features, indicating the sedimentation rate being sufficient to balance the basin subsidence.

#### 6.1.2. Sequence Set A in the Southern Depozone (Tainan basin)

The mid-Oligocene to early Miocene infills (NP24-lower c.NN2) in the Tainan Basin show a two-fold motif of sandstone-mudstone lithology (Figs. 7, 8). A part of this unit or the entire unit has been regarded (e.g., Wu, 1991; Lee et al., 1991, Lee et al., 1993; Tzeng et al., 1996) as accumulating during a rift stage that followed the initial seafloor spreading of the South China Sea at ~30 Ma. The duration for this suggested rift event, however, has been in dispute. Moreover, the stratigraphic architecture of this sandstone-mudstone succession was also unclear. The well-log sequence correlation presented in this study has successfully correlated this unit among the boreholes (see Fig. 8, for example) and linked this unit to its counterpart in the north (Fig. 7). There are three sequences, namely TO0, TO2, and TM0, identified on the basis of bounding unconformity and correlative conformity. The ages for these three sequences were constrained by the bio-horizons.

It should be noted that these sequences have only been drilled at approximately 30 well locations in the Central Uplift Zone of the Tainan Basin (CUZ in Fig. 6). In other areas of the outer margin, their equivalents have been sampled at fewer than 10 well locations. As a result, the

well-log sequence stratigraphy presented below for the sequence set A inevitably draws examples from the Central Uplift Zone.

**6.1.2.1. Sequence TO0.** Sequence TO0 is bounded below by the regional breakup unconformity (base NP24, ~30 Ma) and above by a local erosional unconformity and its correlative conformity (Figs. 7 and 8). The upper sequence boundary formed at the NP24/NP25 boundary (~27.5 Ma). TO0 is a sandstone unit and is informally coined the “Oligocene Transgressive Sandstone” by researchers in CPC Corporation, Taiwan. This sandstone unit is in NP24 (~30–27.5 Ma) and directly overlies lower Cretaceous continental deposits. Huang (1982) tentatively suggested that the biozone of this sandstone unit may extend down to NP23, although NP23 has yet to be recognized. TO0 shows the following features (Fig. 8):

- Its drilled thickness ranges from tens of meters to about 300 m (at the FC7 well, for example) and the thickness generally changes abruptly within a short distance;
- It consists of bioturbated, fine-grained, and calcareous sandstone (Chen, 1993). Coarser-grained sediments have only been found in the lowermost section associated with the occurrence of volcanic gravels (Huang and Yuan, 1996). Also, there is a slightly overall fining-upward trend;
- The paleo-water depth was interpreted to deepen upward from nonmarine at the base to <200 m at the top (Lee et al., 1991) based on the paleoecology of benthic foraminifera. This

- interpretation is further confirmed by the existence of larger foraminifera (Huang and Yuan, 1996) of shallow marine origin;
- (d) An acme zone (labeled as “a” in Fig. 8) with the relative abundance of a nannofossil species, *S. distentus*, is present at the upper portion of this sandstone unit; and
- (e) The upper boundary is either a sharp boundary (i.e., unconformity) separating the thick sandstone from the overlying thick marine mudstone or a gradational contact (correlative conformity) showing a pronounced fining-upward trend. Also, available dipmeter data show an abrupt change of stratal dip across the unconformity (at the FC7 well in Fig. 8, for example) or a gradual decreasing in stratal dip across the correlative conformity (at FC6, for instance).

6.1.2.2. *Sequence TO2*. Sequence TO2 (27.5–21 Ma, NP25 to lower c. NN2) is dominantly a mudstone unit. Its lower boundary is the upper boundary of sequence TO0 and has been described above. The upper boundary is a local erosional unconformity at footwall blocks (e.g., at the FC1 and FC7 wells, Fig. 8) passing laterally into a correlative conformity at hanging wall blocks (e.g., at the FC6 and FC9 wells). Northward toward the basin margin at the EY1 well (Fig. 7), this boundary is characterized by a lithological change from shale/fine-grained sandstone interbeds containing thin limestone layers below to predominantly fine- to coarse-grained sandstones above. It is noted, however, that this upper boundary shows only a subtle change of log patterns across this boundary in the outer margin. Sequence TO2 has the following features (Fig. 8):

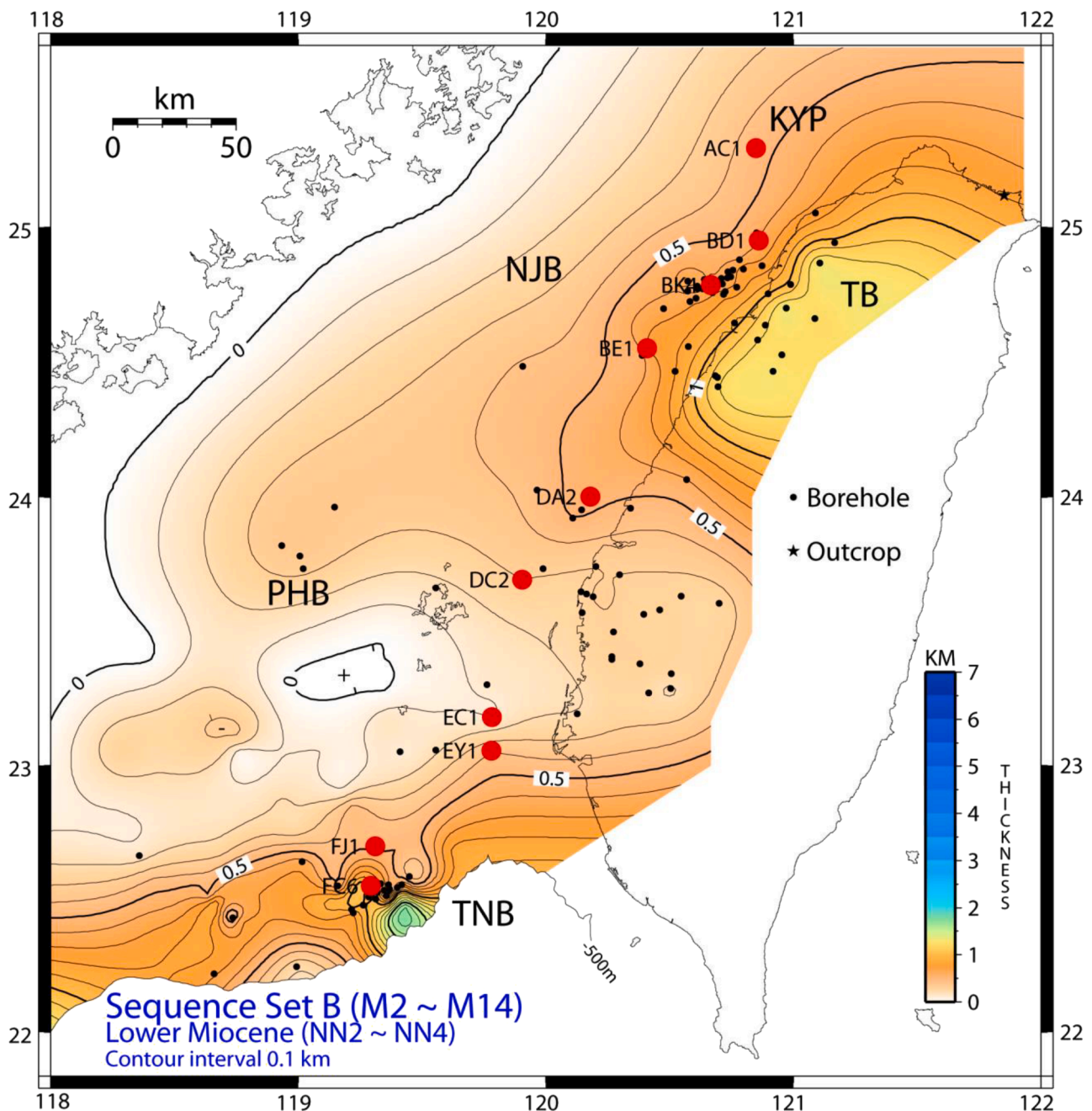


Fig. 9. Sediment isopach of the sequence set B. Red dots show the borehole locations for the north-south well-correlation panel shown in Fig. 10. (For interpretation of the references to color in this figure legend, the reader is referred to the web version of this article.)

- (a) Its thickness varies across fault blocks. It thins over the footwall blocks and thickens over the hangingwall blocks where the maximum drilled thickness is up to 630 m at the FC6 well. It is absent over the horst that was drilled at the FF1 well;
- (b) At the hangingwall blocks, it shows a fining-upward succession (NP25-c.NN1) followed by a coarsening-upward interval (lower c.NN2). In contrast, at the footwall blocks, the sequence is dominated by a coarsening-upward succession with a relatively thin, fining-upward interval at its base;
- (c) In the fining-upward section, it shows a gradual transition from siltstones upward into thick shale with increasing contents of forams and thin limestone beds. The paleo-water depth for the fining-upward sequence was interpreted to be around the interval ~200–500 m (Lee et al., 1991) on the basis of benthic foraminifera; and
- (d) Two acme zones with a relative abundance of nannofossils are present in the fining-upward succession. The lower acme zone (labeled as “b” in Fig. 8), *S. ciperoensis*, occurred in NP25. The upper acme zone (labeled as “c” in Fig. 8, *S. delphix*), occurred in c.NN1 as the most pronounced acme zone in the entire Cenozoic sediments of the Tainan Basin. In the coarsening-upward succession, it shows an increasing content of siltstone and coal fragments with decreasing content of forams. An acme zone (labeled as “d” in Fig. 8 of *C. abisectus*) is present at the lower half of the coarsening-upward trend.

6.1.2.3. Sequence TM0. Sequence TM0 (lower c.NN2) is a marine mudstone unit (Fig. 8). Its lower sequence boundary is the upper sequence boundary of TO2 and it can only be identified on the basis of

the local erosional hiatus at previous footwall blocks as noted above. Elsewhere in the Tainan Basin, the stratigraphic position of the lower boundary can only be approximated. The upper boundary is a surface that separates the mudstone from the overlying thick, and homogeneous marine siltstone bed (Figs. 7, 8). This thick siltstone unit is linked up dip to the lowstand and transgressive systems tracts of M2 in the Taihsi Basin. The deposition of TM0 appears to “level off” the pre-existing horst-and-graben structures in the Tainan Basin (Fig. 8).

6.2. Sequence Set B: Early Miocene (~21–17.3 Ma)

Sequence set B consists of 7 sequences (sequences M2 to M14, Fig. 2) in a duration of ~4 Myr. The lower boundary is the lower M2 sequence boundary which is dated ~21 Ma and is in middle c.NN2 as described in Section 5. The upper boundary is the lower M16 sequence boundary which is in NN4 and is dated ~17.3 Ma by linear interpolation between the ages of the top and base of NN4.

Sediments of sequence set B blanket the study area with slightly larger thickness in preceding rift centers and thinner sediments on basement highs (Fig. 9). This sequence set represents the first major episode of marine transgression since continental breakup (Fig. 10). It comprises a suite of sediments deposited in coastal to shallow-marine environments with a few fluvial and deltaic excursions evident in the proximal setting. A fall in water depth and ensuing pronounced rise in c. NN2 marked the beginning of deposition of the sequence set B. This sea-level cycle led to the accumulation of the lowstand and transgressive systems tracts of M2 that culminated in the development of the *Miogypsina-Lepidocyclina*-Mollusca maximum flooding surface (M-L-M in Fig. 10). This interval serves as one of the regional marker beds in the

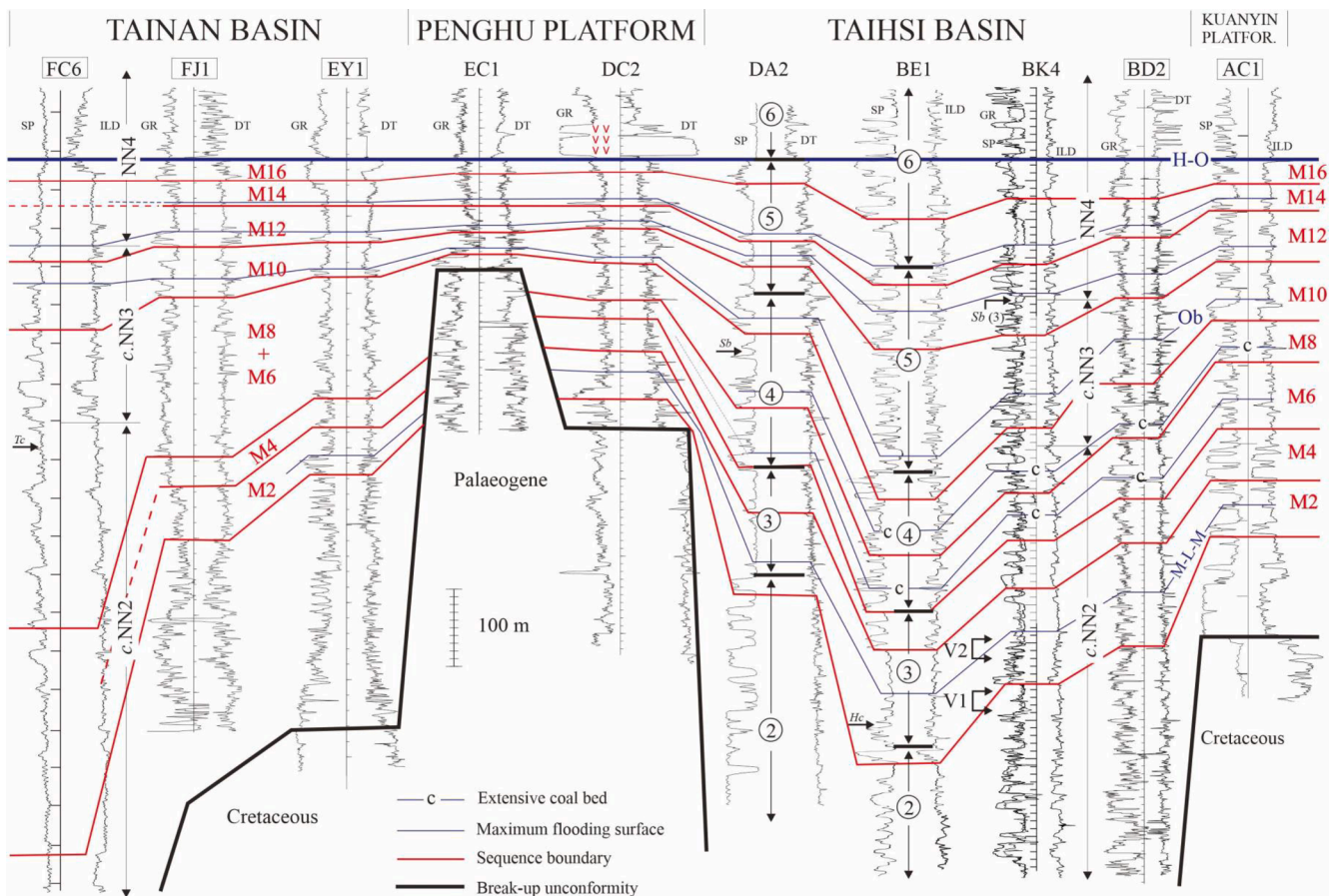


Fig. 10. Sequence variability from inner to outer margin for the sequence set B (see Fig. 10 for well locations. V1 and V2 alongside the BK4 well indicate the equivalent stratigraphic levels for the NW Taiwan basalts that were dated and reported in Juang (1996). Rock formations are numbered as those in Fig. 2. Arrows indicate key occurrences of index nannofossils of the following: Hc: *H. carteri*, Sb: *S. belemnus*, Tc: *T. carinatus*.

west Taiwan basins. Water depth variations following the deposition of M2 were of small magnitude and led to the accumulation of a suite of coastal to shallow-marine sequences (M4 to M14, Fig. 10). Among these sequences, sequences M6 and M8 show more pronounced and prolonged decrease in water depth such that a coal-bearing succession of coastal plain origin was formed in the basin margin in the north (e.g., the Shihti Formation in the Taihsi Basin, Figs. 3, 10). There are several coal seams in sequences M6 and M8. Among these coal beds, two layers are of regional extent which can be correlated downdip for about 100 km (Fig. 10). These two regional coal beds are interpreted as maximum flooding surfaces of sequences M6 and M8, respectively.

The development of the maximum flooding surface of sequence M10 marks resumed marine deposition in the Taiwan region. The maximum flooding surface of M10 is characterized by the rich occurrence of a

foraminiferal species (cf. Huang, 1976; Chinese Petroleum Corporation, 1985), *Operculina bartschii*, at the top of the Shihti Formation. The M10 maximum flooding surface is thus termed the *Operculina bartschii* maximum flooding surface in this study. During this interval of relative deeper water condition, the remaining sequence M10 together with M12 and M14 accumulated in a largely shallow-marine environment.

Equivalent lithostratigraphic units and sequences in the offshore Taihsi Basin are (Figs. 2, 10): (a) Piling Shale (the TST and HST of M2, and M4); (b) Shihti Formation (M6, M8, and the LST plus TST of M10); (c) Peiliao Formation (the HST of M10, M12, and the TST of M14) and; (d) the lower shale member of the Talu Shale (the HST of M14). In onshore northern Taiwan, the equivalent lithostratigraphic units and sequences are: (a) Taliao Formation (the TST plus HST of M2, and M4); (b) Shihti Formation (M6, M8, and the LST plus TST of M10) and; (c)

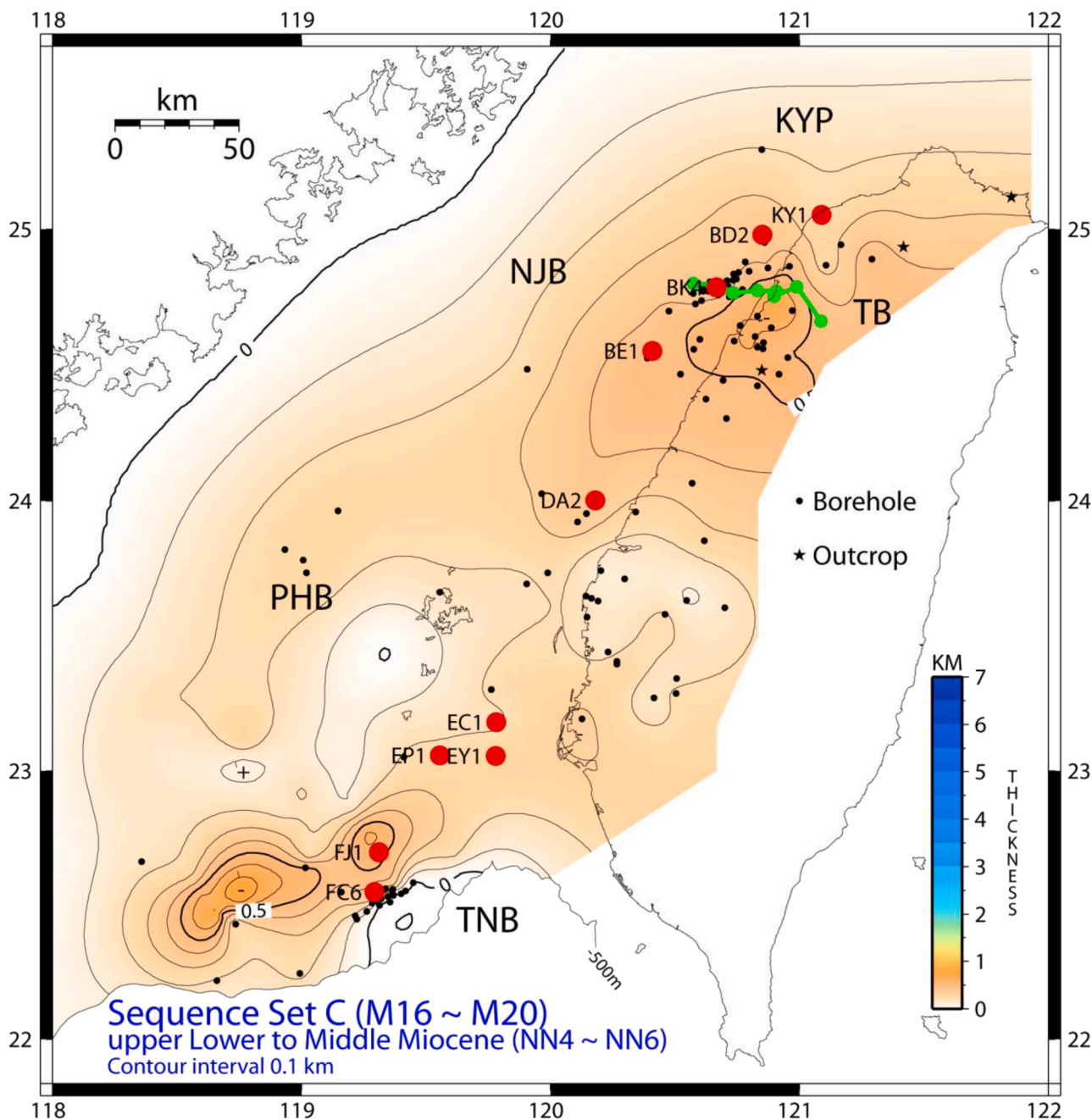


Fig. 11. Sediment isopach of the sequence set C. Red dots show the borehole locations for the north-south well correlation panel shown in Fig. 12. The green line in the Taihsi Basin shows the locations for the well-correlation panel illustrated in Fig. 4. (For interpretation of the references to color in this figure legend, the reader is referred to the web version of this article.)

Peiliao Formation (the HST of M10, M12, M14 and the LST plus TST of M16). Note that the upper boundary of the Peiliao Formation in the offshore and onshore regions is diachronous (see Fig. 4, for example).

6.3. Sequence Set C: Early to Middle Miocene (~17.3–12.5 Ma)

Sequence set C consists of sequences of M16, M18, and M20, and it spans an age around 5 Myr (Fig. 2). The lower boundary is the lower M16 sequence boundary which is dated 17.3 Ma as noted earlier. The upper boundary is the upper M20 sequence boundary (or lower M22 sequence boundary) which is the mid-Miocene unconformity and interpreted as in zone NN6 with an estimated age of ~12.5 Ma (i.e., the base of the Nanchuang Formation, see Section 5). Sediments of sequence set C evenly drape the continental margin with slightly thicker sediments in the preceding rift centers and thinner sediments on basement highs (Fig. 11).

Sequence set C, or sequence M18 in particular, accumulated during the most pronounced transgression throughout the Oligocene-Miocene period in the Taiwan region. This interpretation is based on the following arguments:

- (a) Sediments recovered from the most landward boreholes (i.e., wells in the Penghu Basin (PHB, Fig. 11) show that coal seams are absent in sequence set C but they are prevalent in the remaining Oligocene-Miocene succession in the Penghu Basin. This feature indicates that sediments of sequence set C may have laid down in a marine-influenced environment (see below) which precludes the formation of nonmarine coal beds;

- (b) A few shell horizons were found in upper M16 and M18 sequences in the Penghu Basin wells, suggesting marine influence during the deposition of the above sequences;
- (c) Downdip in the marine realm in northwestern Taiwan, the Talu Shale (equivalent to upper M16 and M18) was reported (e.g., Huang, 1976; Huang, 1989) hosting the most abundant marine micro-fossils for the entire Oligocene-Miocene succession in the Western Foothills e.g., at the Chuhuangkeng section.

The initial phase of this major transgression is marked by the development of the *Heterolepa*-*Orbitoid* maximum flooding surface of M16 (H-O in Figs. 4, 12). This flooding surface developed following the deposition of the lowstand and transgressive systems tracts of M16. Together, the LST, TST, and MFS of M16 sequence form the most widespread marker intervals for Taiwan Cenozoic sediments. Upward across the MFS of sequence M16, there are several characteristic changes in log patterns in the distal marine setting (e.g., in the Penghu Platform and Tainan Basin, Fig. 12). These include: (a) an abrupt increase in the sonic interval transit time (DT) or a decrease in sonic velocity; and (b) an abrupt decrease in resistivity (at FC6, for example). This surface coincides with a strong seismic reflection in the Tainan Basin, and it is used for regional seismic interpretation and coined as “green horizon” by local explorationists.

Following the development of MFS of sequence M16, a local deltaic lobe was developed in the north which showed pronounced progradational and retrogradational parasequence stacking patterns (e.g., Fig. 4). This deltaic succession formed the main part of the Talu Sandstone in the Taihsi Basin. An overall phase of sediment progradation interrupted by a

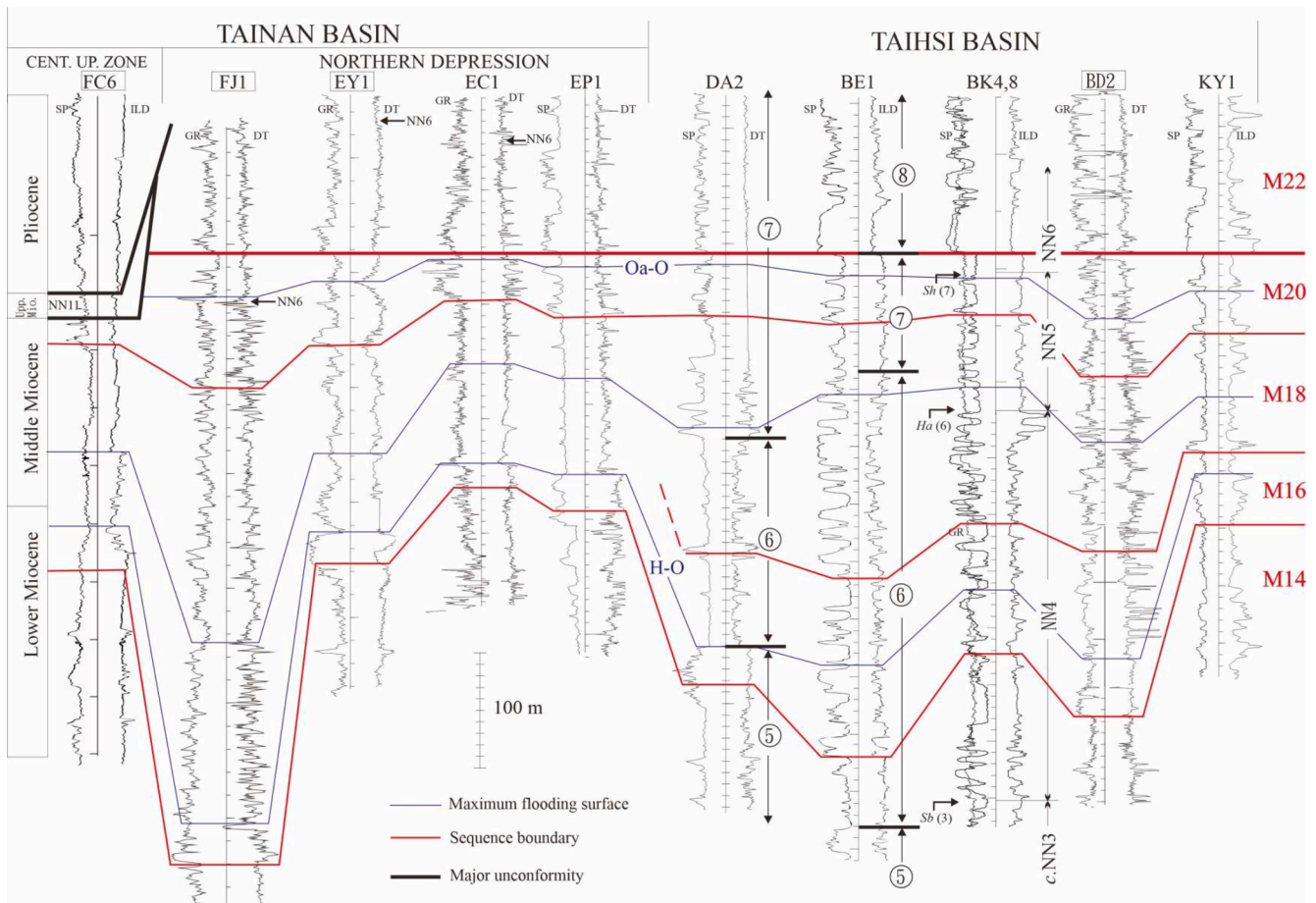


Fig. 12. Sequence variability from inner to outer margin for the sequence set C (see Fig. 11 for well locations and Fig. 4 for another well-correlation panel that aligns in a perpendicular direction to this panel across the Taihsi Basin (TB). The full names for rock formations (numbers) and maximum flooding surfaces are shown in Fig. 2.

sediment retrogradation of short duration (e.g., Fig. 4) concluded the deposition of the sequence set C. This phase of sediment retrogradation formed the transgressive systems tract of sequence M20 which is characterized by the occurrence of *Operculina ammonoides*. The transgressive systems tract of M20 and its *Operculina ammonoides*-*Operculina* maximum flooding surface serve as an additional regional marker bed in the Taiwan region (Fig. 12).

Equivalent lithostratigraphic units and sequences in the offshore Taihsi Basin are (Figs. 2, 4, 12): (a) the Talu Sandstone member and Upper Shale member of the Talu Shale (M16 and the LST plus TST of M18); and (b) Kuanyinshan Sandstone (the HST of M18, and M20). In onshore northern Taiwan: (a) upper Peiliao Formation (the LST and TST

of M16); (b) Talu Shale (the HST of M16 and the LST and TST of M18) and; (c) Kuanyinshan Sandstone (the HST of M18, and M20).

#### 6.4. Sequence Set D: Middle to Late Miocene (~12.5–6.5 Ma)

There are three sequences, M22, M24, and M26 comprising sequence set D (Fig. 2) accumulated within 5 Myr. The lower boundary is the lower M22 sequence boundary which is the base of the Nanchuang Formation and is dated ~12.5 Ma (see Section 5). The upper boundary is the top Nanchuang Formation which corresponds to the top of the M26 sequence boundary or the basal foreland unconformity. It is dated ~6.5 Ma according to Lin et al. (2003).

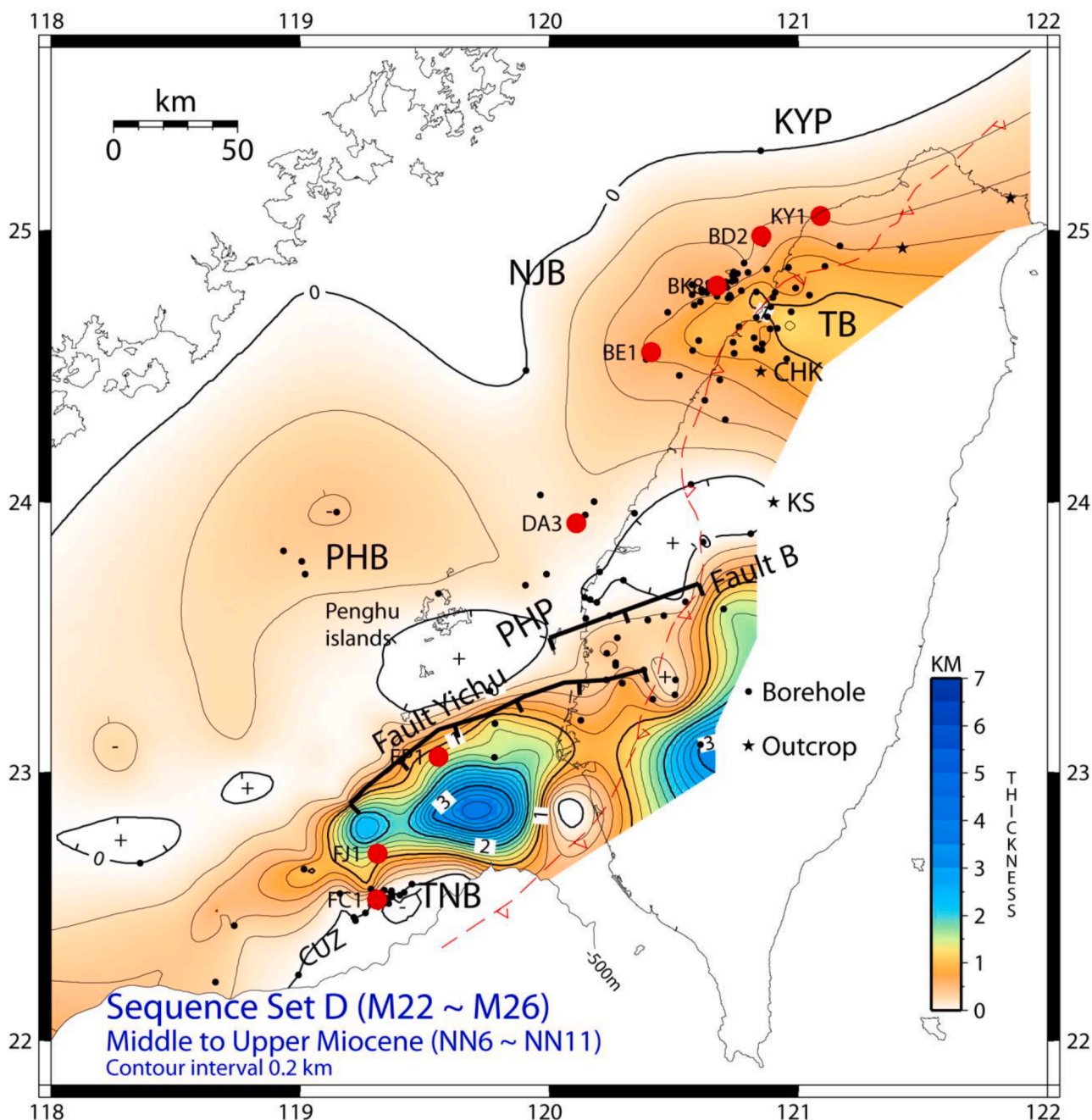


Fig. 13. Sediment isopach of the sequence set D (Lin et al., 2003). Sediments of the sequence set D were accumulated in two, north and south, rift centers separated by the NE-trending rift flank, the Penghu Platform (PHP). Also shown are the two main rift border-faults, the Yichu and B Faults. The present-day thrust front is shown as a dashed and barbed line. The isopach map clearly shows that the late Miocene Penghu rift flank extended across the present-day thrust front and reached, at least, to the western flank of the Hsuehsan Range (for example at the Kuohsing area, denoted as KS). Red dots are locations of wells shown in the correlation panel of Fig. 14. (For interpretation of the references to color in this figure legend, the reader is referred to the web version of this article.)

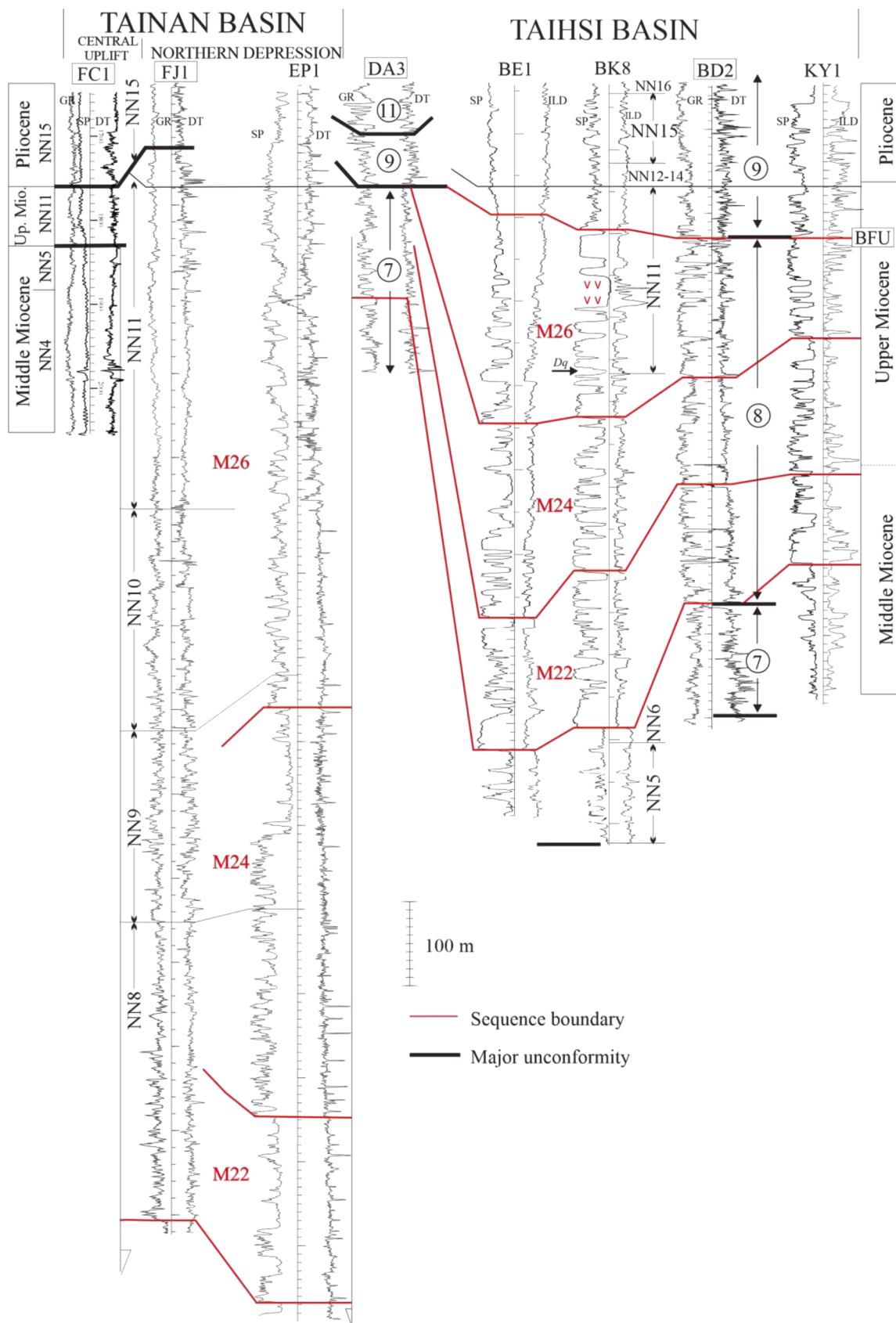


Fig. 14. Sequence variability from inner to outer margin for the sequence set D. The arrow alongside the BK8 well indicates the occurrence of an NN11 index fossil, *D. quinquaramus*, Dq, identified from sidewall core samples. Numbered lithostratigraphic units are the same as shown in Fig. 2.

The sediment isopach of the sequence set D (Fig. 13) is segmented by the NE-trending Penghu Platform, a rift flank that developed during the deposition of the sequence set D. A relatively thin succession of fluvial to paralic sediments was ponded in the depocenters to the north of the Penghu Platform. In contrast, a thick marine mudstone interval accumulated to the south of the Penghu Platform, in the Northern Depression of the Tainan Basin. The Northern Depression is further bordered to its south by the Central Uplift Zone (CUZ) on which sediments of the sequence set D are largely missing. A significant and prolonged drop in relative sea-level at about 12.5 Ma brought about most of the northern depozone to a nonmarine to coastal realm, while marine conditions still prevailed in the Tainan Basin. This depositional setting lasted until about 6.5 Ma when an overall marine transgression was initiated. The initial relative sea-level fall at ~12.5 Ma formed the lower M22 sequence boundary which is characterized by thick fluvial sandstones overlying marine sediments in the north (Figs. 12, 14).

The largely nonmarine successions in the north can be grouped into three sequences of M22, M24, and M26, respectively, on the basis of the cyclic development of three fining-upward successions (Fig. 14). The sequence boundary in this succession can be recognized as a surface that separates thick mudstone below from the lateral extensive and amalgamated fluvial channel sandstones above. These three nonmarine to coastal sequences, M22, M24, and M26, identified in the north, were then correlated to the marine realm in the south across the Penghu Platform. The correlation of the M24 and M26 across the Penghu Platform is only meant to be tentative because of the lack of adequate biostratigraphic controls in the Taihsi Basin together with the absence of continuous stratal marker beds across the Penghu Platform.

The occurrence of marine forams at a downdip location at the Chu-huangkeng section (CHK in Fig. 13) provides insight for the relative amplitude of sea-level fall during the deposition of sequences M22, M24, and M26. At this location, Huang (1989) pointed out that the middle Nanchuang Formation (approximately equivalent to M24) is barren of foraminifera, whereas upper and lower parts of the Nanchuang Formation contain benthic foraminifera of marsh to inner neritic origin. The middle Nanchuang Formation (M24) therefore represents sediments accumulated during the most pronounced progradation during the deposition of the Nanchuang Formation. Further south along the depositional strike at the Penghu islands (Fig. 13), Lee (1994) reported that the thickest paleosol preserved in the upper Miocene Penghu basalts was formed at about 10 Ma on the basis of the ages of basalts that enclose the paleosol. This age is in accord with the estimated age, ~10.5 Ma, for the lower M24 sequence boundary in the Taihsi Basin by linearly interpolating between the ages for the top (6.5 Ma) and base (12.5 Ma) of the sequence set D.

## 7. Discussion

### 7.1. Tectonic development and sedimentary responses

Backstripping analysis (Lin et al., 2003) shows that two phases of rapid subsidence, related to lithospheric extension, occurred during the periods ~30–21 Ma and 12.5–6.5 Ma, corresponding to the deposition of sequence sets A and D, respectively. In between these two extensional events, regional thermal subsidence prevailed during ~21–12.5 Ma, with the deposition of sequence sets B and C. The contrast of tectonic events for our studied sequence sets, therefore, warrants us to discuss the tectonic controls on stratigraphic sequence developments, and this aspect of discussion has been of strong interest in the literature (e.g., Ravnas and Steel, 1998; Gawthorpe and Leeder, 2000; Zecchin et al., 2006).

#### 7.1.1. Sequence Set A: Rifting-related Deposition, Oligocene to Early Miocene (~30–21 Ma)

As pointed out by Lin et al. (2003) the anomalously rapid, post-breakup subsidence following the continental breakup at ~30 Ma is

more evident in the outer margin (i.e., Tainan Basin) than that in the inner margin (i.e., Taihsi Basin). Apparently, normal faulting occurred during the interval ~30–21 Ma in the outer margin (e.g., the Tainan Basin, Fig. 8) and accompanied much of this rapid subsidence phase. In contrast, the rapid subsidence in the inner margin was associated with a lack of normal faulting as evidenced by the “steer’s head” basin geometry (Fig. 5) and a gradual thickening toward the former rift center and thinning toward the basin margin. These features are characteristic features for basins dominated by post-rift thermal subsidence (e.g., White and McKenzie, 1988).

The local normal faulting in the outer margin led to the development of small horsts and grabens in the Tainan Basin as early as during NP24 (~30–27.5 Ma) and resulted in the accumulation of the fault-bounded TO0 sequence i.e., the “Oligocene Transgressive Sandstone”; while elsewhere in the west Taiwan basins experienced an erosional or non-depositional episode. During NP25, seawater transgressed over the former rift center in the Taihsi Basin in the inner margin and laid down the first post-breakup sediments (sequence O2) unconformably on the Paleogene *syn*-rift infills. In the outer margin, this phase of marine transgression coincided more or less with an enhanced rifting episode. The enhanced rifting led to the accumulation of a strong transgressive interval at the hangingwall blocks, which forms the transgressive system tract of sequence TO2 in the outer margin. It is worth noting that NP25 marine fossils have also been found in two wells in the Zhu-2 depression on the southwest of the South China margin (Huang, 1997). These NP25 fossils are the oldest Cenozoic marine fossils identified there (i.e., at the BY7-1-1 and PY33-1-1 wells). This shows that the NP25 transgression may have affected much of the South China margin and this transgression may mark the first marine transgression in the SW portion of the South China margin. An ensuing sea-level drop during the interval ~24–21 Ma brought the inner margin in the Taiwan region into a nonmarine setting and accumulated two fining-upward and cyclic sequences, O4 and M0. In the outer margin, rifting continued during this stage and marine shales were ponded in fault-bounded troughs. Biostratigraphic data and sequence correlations from inner to outer margins show that the normal faulting in the outer margin exerted strong controls on the sedimentation and sequence development during the deposition of the sequence set A. The normal faulting also resulted in the variations on the timing of sequence boundaries across the margin. For example, the lower O4 sequence boundary in the inner margin is absent from the outer margin (Figs. 2, 7).

In particular, the sequence set A in the Tainan Basin also bears an important economic interest for hydrocarbon exploration although its stratigraphic architecture was previously poorly understood. A further discussion on the development of the sequence set A in the outer margin is therefore warranted as described below. The sequence set A in the Tainan Basin is interpreted, in this study, as the record of a consecutive, two-stage rifting event (Fig. 8). During the initial rift stage (~30–27.5 Ma, NP24), extension was mild such that the rate of fault-controlled subsidence was slightly higher than the sedimentation rate. This led to the development of a nearshore to shallow-marine environment in a rift setting on top of the Mesozoic basement where the relatively homogeneous “Oligocene Transgressive Sandstone” or sequence TO0 (NP24) was ponded in a series of small fault blocks.

As rifting progressed, normal faulting concentrated on fewer faults, leading to the development of the second, more intense, rift stage (~27.5–21 Ma, NP25-lower c.NN2) and the deposition of sequences TO2 and TM0. During the early, second rift phase (~27.5–24, NP25-c.NN1), a rapid subsidence rate at the hangingwalls (at the FC6, 8, and 9 wells in Fig. 8, for example) outpaced the rate of sedimentation and resulted in a transgression and reduction in sediment flux to rift centers. An upper bathyal environment (300–500 m of paleo-water depths, Lee et al., 1991) was thus formed and a strong transgressive succession deposited. The hangingwall subsidence was also accompanied by fault-block rotation as indicated by the dipmeter data showing an upward decreasing in structural dip in the strong transgressive interval (e.g., at

the FC6 well, Fig. 8). Coeval to the subsidence at the hangingwall blocks was uplift at the footwall blocks/rift shoulders (at the FF1, FC1, and FC7 wells, for example). The uplifted footwall blocks may have elevated to a shallower water depth or may have emerged as islands where the previously deposited TO0 sequence was partly eroded. This uplift and erosional event at the footwall blocks at ~27.5 Ma (the NP24/NP25 boundary) created local unconformity that shows a dramatic lithologic change and a discontinuity in structural dips (at FC7, for example) across the unconformity. Following the development of the NP24/NP25 footwall unconformity, a transgression soon inundated the entire region except for the region at the FF1 well. The rift climax may be interpreted to coincide with the transition from the transgressive interval below to the regressive succession above at mid-c.NN1. This transition also roughly corresponds to the *Sphenolithus delphix* acme zone (labeled as “c” in Fig. 8). The thick regressive interval with dominant shale and siltstone may be regarded as infilling the topography largely created during the previous rifting event. A shallowing and progradational stratigraphic signature was thus developed which forms the highstand systems tract of sequence TO2.

Faulting activities waned during the late stage of the deposition of the sequence set A in the Tainan Basin although marine conditions still prevailed in this region. As such, the relative sea-level fall that led to the development of the lower M0 sequence boundary in the inner margin (Fig. 7) may also have controlled the development of the lower TM0 sequence boundary in the outer margin. Finally, the deposition of TM0 in the outer margin appears to passively “fill” up the existing rift topography.

#### 7.1.2. Sequence Sets B & C: Thermal Subsidence-related Deposition, Early to Middle Miocene (~21–12.5 Ma)

Sediments of sequence sets B and C evenly blanketed the west Taiwan basins (Figs. 9, 11), reflecting that the basin subsidence was driven by regional thermal cooling of the lithosphere following the previous rift event(s). Backstripping analysis (Lin et al., 2003) also indicates a relatively slow (thermal) subsidence of the entire west Taiwan basins during the deposition of sequence sets B and C.

These two sequence sets recorded an overall marine transgression in the Taiwan region during the interval ~21–12.5 Ma (mid-c.NN2 to lower NN6). The first pronounced transgression was marked by the development of the *Miogyopsina-Lepidocyclus-Mollusca* (M-L-M) maximum flooding surface of sequence M2. A later regression of short duration led the fluvial system to prograde basinward and deposited coal-bearing sequences of M6 and M8 in the inner margin and their coeval marine sequences in the downdip setting. An ensuing transgression resulted in the development of the *Operculina bartschii* maximum flooding surface of M10 (Ob in Fig. 10) and resumed marine conditions in much of the west Taiwan basins. It was during the deposition of M10, that much of the previously emerged Penghu Platform became submerged and started to receive sediments (e.g., Fig. 10).

Following a series of small-scale rise and fall of relative sea-level which laid down sequences M12 and M14, a major phase of transgression was marked by the *Heterolepa-Orbitoid* (H-O) maximum flooding surface of sequence M16. The marine transgression, however, did not reach its maximum until the development of the maximum flooding surface of sequence M18. The maximum transgression in the Taiwan region correlates well with the “Mid-Miocene Climatic Optimum” (CO in Fig. 15), indicating that the Taiwan Miocene maximum transgression is a global signature (see Section 7.2 for further discussion). The maximum transgression was then followed by a sediment progradational phase during the deposition of sequence M18. This phase was interrupted by a short period of transgression of small magnitude during late NN5 that formed the transgressive systems tract and the *Operculina ammonoides-Operculina* (Oa-O) maximum flooding surface of M20.

#### 7.1.3. Sequence Set D: Rift-related Deposition, Middle to Late Miocene (~12.5–6.5 Ma)

The backstripping analysis of Lin et al. (2003) has shown that the deposition of the sequence set D was accompanied by rapid subsidence in rift centers and non-deposition or uplift in the rift flanks. The spatial distribution of the rift centers and flanks is evident from the isopach map (Fig. 13) of the sequence set D with thick sediments denoting rift centers and thin intervals representing rift flanks. To the north of the Penghu Platform, the thickness of sequence set D thickens toward the former Paleogene *syn*-rift depocenter and thins toward the Penghu Platform. Stratigraphic correlation in the Taihsi Basin shows that the strata of the sequence set D was segmented by *syn*-sedimentary normal faults as shown in Lin et al. (2003). Thickness change for the sequence set D (Fig. 12 of Lin et al., 2003) in between closely spaced wells is in the order of <500 m which is, however, an order of magnitude less than that in the Tainan Basin (Fig. 14). This feature reflects that the lithosphere was less stretched in the inner margin than in the outer margin during the late Miocene.

The timing for the initial late Miocene rifting may be inferred by the abrupt thickness increase of sequence M20. Fig. 4 shows one of the examples: an abrupt M20 thickness increase occurs between wells UNG1 and HS1 in the Taihsi Basin, suggesting that the late Miocene normal faulting (or rifting) probably initiated during the deposition of the highstand systems tract of M20. The inferred timing for initial rifting is slightly older than the development of the M22 sequence boundary. For simplicity, the age of the lower M22 sequence boundary, ~12.5 Ma, is taken to be the age for the initial rifting. This rift episode, from 12.5 to 6.5 Ma, was also accompanied by basaltic eruptions which were especially active in the vicinity of the Penghu islands and northern Taiwan.

#### 7.2. Eustatic control on the development of the Oligocene-Miocene passive margin sequences

Eustasy is commonly inferred (e.g., Posamentier and Vail, 1988) to be the dominant controlling factor on sequence and systems tract development on a passive margin. It is therefore desirable to correlate the Taiwan Oligocene-Miocene passive-margin record to the inferred “global” sea-level records in a view to test the above hypothesis. To this end, paleontologic data have been used to bracket the ages of the individual sequences in the west Taiwan basins. It is noted, however, that biostratigraphic data are not detailed enough at present to correlate precisely to the time scale and inferred eustatic records.

As many workers have pointed out (e.g., Browning et al., 1996) that large ice sheets have existed in Antarctica since at least the late middle Eocene, the waning and waxing of continental ice-sheets and hence glacioeustasy have been proposed to be a primary control on the formation of sequence boundary since ~42 Ma (Miller et al., 1998). The deep-sea  $\delta^{18}\text{O}$  record provides a proxy for glacioeustasy. An increase in  $\delta^{18}\text{O}$  indicates an glacioeustatic fall and vice versa. Fig. 15 compares the Taiwan record to the global deep-sea oxygen isotope data of Zachos et al. (2001), oxygen isotope maximums of Miller et al. (1998), and the inferred eustasy of Haq et al. (1988). From this comparison, one finds the following points.

- During the mid-Early to Late Miocene (~21–5 Ma), the Taiwan relative sea-level and the glacioeustasy inferred by the oxygen isotope record were in broad agreement. There is an overall ~21–15 Ma transgression followed by ~15–6 Ma regression.
- The Middle Miocene Climatic Optimum (Flower and Kennett, 1994; Zachos et al., 2001, CO in Fig. 15) and the Monterey carbon-isotope excursion (Cheng et al., 2004; Diester-Haass et al., 2009; Vincent and Berger, 1985) correspond to the gradual Taiwan Miocene maximum transgression, with its maximum transgression occurring at ~16 Ma. Notably the dated ages (16.9–13.5 Ma) for the Monterey event (Holbourn et al., 2007) is broadly consistent with the depositional age of sequence set C

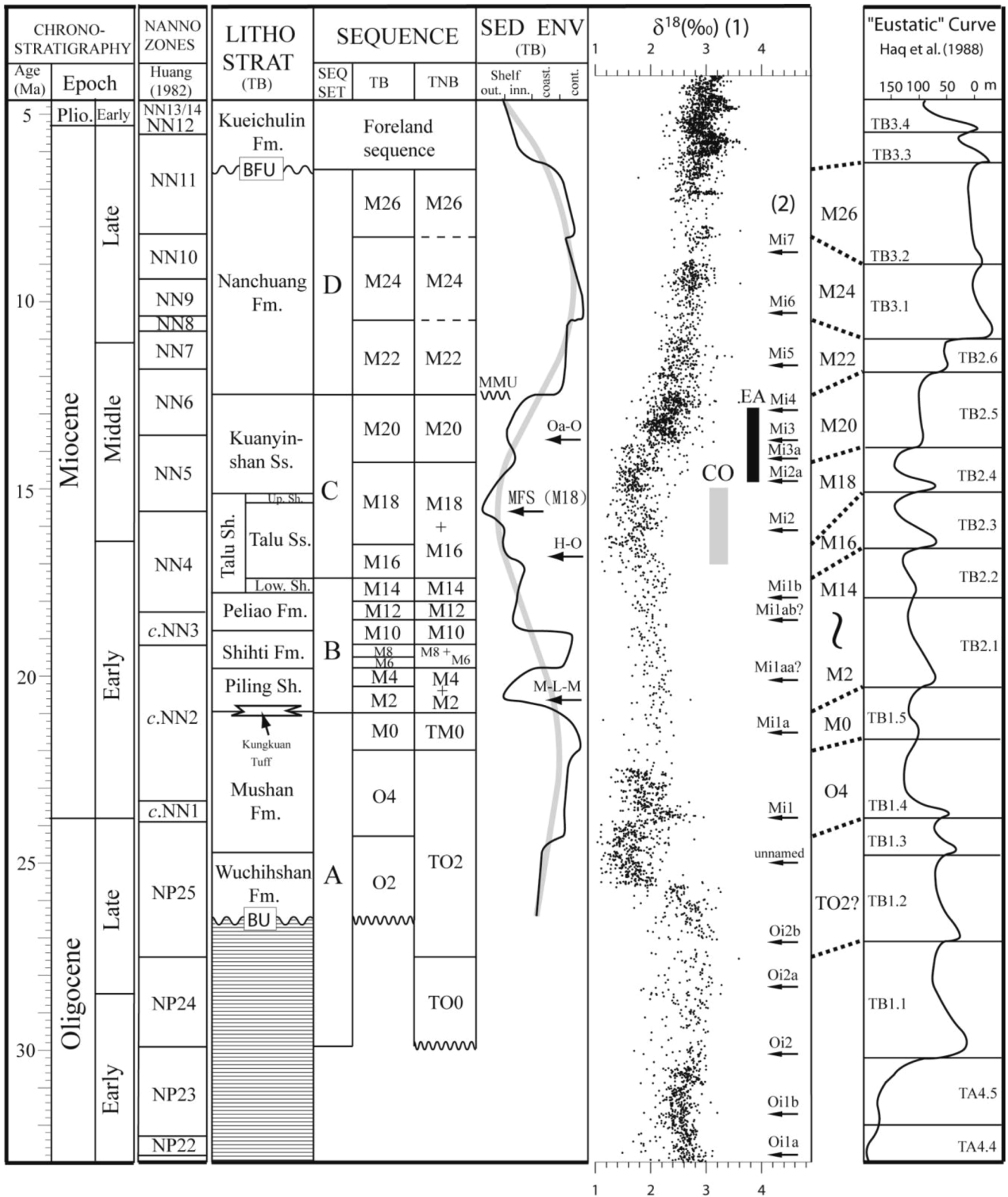


Fig. 15. A tentative correlation of the Taiwan Oligocene-Miocene sequences with the oxygen isotope records (1: Zachos et al., 2001),  $\delta^{18}O$  maximums (2, indicated by arrows: Miller et al., 1998) and inferred "eustatic" sea-level of Haq et al. (1988). The sedimentary environment for the Oligocene-Miocene succession in the Taihsi Basin is a proxy for paleo-water depth. The thick gray line shows the averaged paleo-water depths. The ages for the third-order cycles of Haq et al. (1988) are modified according to Miller et al. (1998). The Cenozoic time scale is according to Berggren et al. (1995). The durations for the Mid-Miocene Climatic Optimum (CO) and the East Antarctic ice-sheet (EA) are from Zachos et al. (2001) and Flower and Kennett (1994), respectively. BU: Breakup unconformity, BFU: Basal Foreland Unconformity, MMU: Mid-Miocene Unconformity.

(sequences M16, M18, M20) during 17.3–12.5 Ma. The MFS of sequence M18 occurs near the boundary of zones NN4 and NN5 (see Fig. 4), around 16 Ma, representing the most widespread marine transgression during the Oligocene and Miocene Epochs in the study area. This age coincides with the lowest  $\delta O^{18}$  value, indicating warmest temperature and highest global sea level during the Miocene (Miller et al., 1987). During the deposition of sequences M16 and M18 (~17.4–14.2 Ma) and the Miocene Climatic Optimum, extreme continental weathering and erosion in the Asian continents was inferred to occur during ~17–15 Ma from studies of ODP cores in the South China Sea (Wan et al., 2009). The overall regressive trend of the sequence set D (i.e., Nanchuang Formation) in the Taihsi Basin during late middle to Late Miocene is in agreement with a long term increase in  $\delta O^{18}$  values (inferred eustatic lowering). Particularly, following the maximum transgression at ~16 Ma, the overall progradational packages of sequences M18 and M20 coincides with the growth of the East Antarctic ice-sheet during 14.8–12.9 Ma (shown as EA in Fig. 15) according to Flower and Kennett (1994). The major unconformity that bounds the base of the sequence set D (i.e. the lower sequence boundary of sequence M22) and occurred within the biostratigraphic zone of NN6, most likely correlates to the “Mid-Miocene Unconformity” found elsewhere in the passive margins such as in the North Sea (Huuse and Clausen, 2001).

- (c) The number of the Taiwan sequences (TO0 to M26) and the duration for individual sequences are similar to the third-order cycles of Haq et al. (1988) (i.e., TB1.1 to TB3.2) with the exception of the lower Miocene sequence set B (see below).
- (d) The lower Miocene sequence set B consists of seven sequences, M2 to M14, that are correlative to two, TB2.1 and TB2.2, third-order cycles. The average duration for the above individual Taiwan sequences is 528 Kyr, a duration falling at the lower bound of the third-order eustatic cycle (i.e., 0.5–3 Myr). The significance of these sequence of short duration is uncertain. Nevertheless, an orbital-forcing mechanism for driving the development of these sequences may be a likely explanation judging from the observation that the average duration for these sequences is close to the ~410 Kyr eccentricity periodicity of the Milankovitch cycle.
- (e) During the mid-Oligocene to mid-Early Miocene (~30–21 Ma) the paleo-water depths and the inferred glacioeustasy from oxygen isotope were in opposite positions although the ages for the Taiwan sequence boundaries roughly correspond to the third-order cycles of Haq et al. (1988). During the above time interval, there was a regression episode in Taiwan versus transgression phase for the inferred eustasy.

The danger of miscorrelation of the Taiwan sequences with the glacioeustasy and the eustatic cycles of Haq et al. (1988) and Miller et al. (1998) is ever present because of the time resolution problem on one hand and the masking effects caused by local tectonism and sedimentation on the other. Permitting minor phase shifts to be reconciled by the masking effects of local geological processes and inadequacy in biostratigraphic resolution, a general correlation of the Taiwan sequence boundaries with the eustatic cycles is obvious for sequences M2 to M26. It therefore appears that eustasy may have been the dominant control on the Taiwan Miocene stratigraphic development since at least ~21 Ma. The deposition of sequence set A during ~30–21 Ma and possibly sequence set D in the outer margin during the late Miocene, however, appears to have been strongly modulated by local sedimentary factors (e.g., rates of basin subsidence, sediment supply and basin physiography etc.). This is evidenced by, for example, the diachronous sequence development across the passive margin together with the local regressive signature vs. overall eustatic transgression during the interval ~30–21 Ma (Fig. 15).

The rate of basin subsidence affects the synchronicity or diachronicity

of the sequence boundary development, as it is the relative sea-level fall (a combination of subsidence and eustasy) that drives the formation of a sequence boundary. As a result, in basins with significantly differing rates of subsidence undergoing the same eustatic sea-level fall with a constant sedimentation rate, sequence boundary formation may not be synchronous or may not even occur. In contrast, the age of the sequence boundaries will only be synchronous (within the limit of biostratigraphic resolution) if rates of sea-level fall are much greater than the rates of subsidence in all basins being considered. The above situations are exemplified by the development of the Taiwan Oligocene-Miocene sequences. Diachronous sequence development was found during post-breakup extension, particularly the deposition of the sequence set A. For example, during ~30–21 Ma, there was a phase of rapid subsidence (Lin et al., 2003) accompanied by normal faulting in the outer margin (Fig. 8). In this depositional setting, differing rate of basin subsidence across the passive margin is expected. As a consequence, the development of the inner-margin sequences, O2 and O4, is not coeval to TO0 and TO2 in the outer margin (Fig. 2). On the contrary, sequence sets B and C (Figs. 2, 10, 12) can be correlated inter-basinally, indicating a “synchronous” sequence development within the limit of the available biostratigraphic resolution. The synchronicity of sequence development may be regarded as the result of the relatively slow and uniform rate of basin subsidence (Lin et al., 2003) that was far exceeded by the rate of eustatic fluctuations across the passive margin during the accumulation of sequence sets B and C.

Moreover, the basin physiography also exerts control on the distribution of sedimentary facies. The prime examples from Taiwan are, again, the deposition of the Taiwan sequence sets A and D. During the deposition of these two sequence sets in the intervals of ~30–21 Ma and ~12.5–6.5 Ma, respectively, the Penghu Platform was uplifted as an emergent rift flank separating the north and southern depocenters (Figs. 6, 13). As a result, the rift flank (i.e., the Penghu Platform) served as a sediment “barrier” that effectively trapped the coarse sediments in the northern depocenter while marine fines were ponded in the south depocenter (Figs. 7, 14).

## 8. Conclusions

The Oligocene-Miocene passive-margin succession in Taiwan is divided into 16 stratigraphic sequences. These 16 sequences can be grouped into four (A, B, C, D) sequence sets. Sequence sets B and C blanketed the west Taiwan basins with relatively uniform thickness deposited during thermally-driven subsidence. Sequence sets A and D, however, thickened into fault-bounded troughs, recording two extensional events that were especially active in the outer margin (e.g., the Tainan Basin). These four sequence sets (A, B, C, D) correspond to depositional ages of ~30–21 Ma, ~21–17.3 Ma, ~17.3–12.5 Ma, ~12.5–6.5 Ma, respectively.

During mid-Early to Middle Miocene (~21–12.5 Ma), all the basins and platforms experienced tectonic quiescence. Stratigraphic sequences can be correlated inter-basinally. In particular, three maximum flooding surfaces, namely *Miogypsina-Lepidocyclina*-Mollusca (sequence M2), *Heterolepa*-Orbitoid (M16), and *Operculina ammonoides-Operculina* (M20) exist pervasively in the study area. These three stratal surfaces serve as good marker beds for future stratigraphic study in this area.

There is a good correlation between the Taiwan Oligocene-Miocene sequences and the glacioeustasy, indicating that transgressive-regressive events evident in these sequence sets likely reflect major global sea-level events. The deposition of the sequence set A during ~30–21 Ma and possibly the sequence set D in the outer margin during the late Miocene, however, appears to have been strongly modulated by extensional tectonics and local sedimentary factors (e.g., rates of basin subsidence, sediment supply and basin physiography, etc.).

## CRediT authorship contribution statement

**Andrew T. Lin:** Conceptualization, Methodology, Funding acquisition, Formal analysis, Writing - review & editing. **Chih-Cheng Yang:** Data curation, Formal analysis. **Ming-Huei Wang:** Data curation, Formal analysis. **Jong-Chang Wu:** Data curation, Formal analysis.

## Declaration of Competing Interest

The authors declare that they have no known competing financial interests or personal relationships that could have appeared to influence the work reported in this paper.

## Acknowledgements

This work was supported by CPC Corporation (grant number FEA0711033) and Ministry of Science and Technology, Taiwan (grant numbers 105-3113-E-008-009, 108-2116-M-008-002).

## Appendix A. Supplementary material

Supplementary data to this article can be found online at <https://doi.org/10.1016/j.jseas.2021.104765>.

## References

- Aitken, J.F., Flint, S.S., 1995. The application of high-resolution sequence stratigraphy to fluvial systems – a case study from the Upper Carboniferous Breathitt Group, eastern Kentucky, U.S.A. *Sedimentology* 42, 3–30.
- Berggren, W.A., Kent, D.V., Swisher III, C.C., Aubry, M-P., 1995. A revised Cenozoic geochronology an chronostratigraphy. In: Berggren, W.A., Kent, D.V., Aubry, M-P., Hardenbol, J. (Eds.), *Geochronology Time Scales and Global Stratigraphic Correlation*. Society of Economic Paleontologists and Mineralogists Special Publication 54, pp. 129–212.
- Briaies, A., Patriat, P., Tapponnier, P., 1993. Updated interpretation of magnetic anomalies and seafloor spreading stages in the South China Sea – implications for the Tertiary tectonics of Southeast Asia. *J. Geophys. Res.* 98 (B4), 6299–6328.
- Browning, J.V., Miller, K.G., Pak, D.K., 1996. Global implications of Eocene greenhouse and doubt house sequences on the New Jersey coastal plain: the icehouse cometh. *Geology* 24, 639–642.
- Browning, J.V., Miller, K.G., Sugarman, P.J., Kominz, M.A., McLaughlin, P.P., Kulpecz, A.A., 2008. 100 Myr record of sequences, sedimentary facies and sea-level change from Ocean Drilling Program onshore boreholes, U.S. Mid-Atlantic coastal plain. *Basin Res.* 20, 227–248.
- Browning, J.V., Miller, K.G., Sugarman, P.J., Barron, J., McCarthy, F.M.G., Kulhanek, D. K., Katz, M.E., Feigenson, M.D., 2013. Chronology of Eocene-Miocene sequences on the New Jersey shallow shelf: Implications for regional, interregional, and global correlations. *Geosphere* 9, 1434–1456.
- Cataneanu, O., 2017. Chapter 1: Sequence stratigraphy: Guidelines for a standard methodology. In: Montenari, M., Steffensen, J.P., Singer, B., Erba, E., Raymo, M., Barker, S. (Eds.), *Stratigraphy & Timescales* 2, pp. 1–57.
- Chang, S.S.-L., Chi, W.-R., 1983. Neogene nannoplankton biostratigraphy in Taiwan and the tectonic implications. *Petrol. Geol. Taiwan* 19, 93–147.
- Chen, Y.-T., 1993. A review of the depositional model and lead area of the Oligocene Sandstone in the Tainan basin, offshore Taiwan. *Petrol. Geol. Taiwan* 28, 269–288.
- Cheng, X., Zhao, Q., Wang, J., Jian, Z., Xia, P., Huang, B., Fang, D., Xu, J., Zhou, Z., Wang, P., 2004. Data report: Stable Isotopes from Sites 1147 and 1148. In: Prell, W. L., Wang, P., Blum, P., Rea, D.K., Clemens, S.C. (Eds.), *Proceedings of the Ocean Drilling Program, Scientific Results* vol. 184, pp. 1–12.
- Chi, W.-R., 1981. The biohorizons of the *Operculina* Limestone, Orbitoid Limestone, and Mollusca Limestone in the subsurface sediments of the Peikang-Yunlin area. *Ti-Chih* 3, 63–71 (in Chinese).
- Chinese Petroleum Corporation, 1985. Tertiary Unconformities, Magmatism, and the Sedimentary Basin Evolution in the Taiwan Region. Offshore Petroleum Exploration Division. Chinese Petroleum Corporation, Taiwan (in Chinese).
- Chou, J.-T., 1973. Sedimentology and paleogeography of the Upper Cenozoic System of western Taiwan. *Proc. Geol. Soc. China* 16, 111–143.
- Christie-Blick, N., 1991. Onlap, offlap, and the origin of unconformity-bounded depositional sequences. *Mar. Geol.* 97, 35–56.
- Cross, T.A., 1988. Controls on coal distribution in transgressive-regressive cycles, Upper Cretaceous, Western Interior, U.S.A. In: Wilgus, C.K., Hastings, B.S., Ross, C.A., Posamentier, H.W., van Wagoner, J., Kendall, C.G.S.C. (Eds.), *Sea-level Changes: An Integrated Approach*. Society of Economic Paleontologists and Mineralogists Special Publication 42, pp. 371–380.
- Chung, S.-L., Sun, S.-S., Tu, K., Chen, C.-H., Lee, C.-Y., 1994. Late Cenozoic basaltic volcanism around the Taiwan Strait, SE China: Product of lithosphere-asthenosphere interaction during continental extension. *Chem. Geol.* 112, 1–20.
- Diester-Haass, L., Billups, K., Gröcke, D.R., François, L., Lefebvre, V., Emeis, K.C., 2009. Mid-Miocene paleoproductivity in the Atlantic Ocean and implications for the global carbon cycle. *Paleoceanography* 24, PA1209. <https://doi.org/10.1029/2008PA001605>.
- Flower, B.P., Kennett, J.P., 1994. The middle Miocene climatic transition: East Antarctic ice sheet development, deep ocean circulation and global carbon cycling. *Paleogeogr. Paleoclimatol. Paleoecol.* 108, 537–555.
- Gawthorpe, R.L., Leeder, M.R., 2000. Tectono-sedimentary evolution of active extensional basins. *Basin Res.* 12, 195–218.
- Haq, B.U., Hardenbol, J., Vail, P.R., 1988. Mesozoic and Cenozoic chronostratigraphy and cycles of sea-level change. In: Wilgus, C.K., Hastings, B.S., Ross, C.A., Posamentier, H.W., van Wagoner, J., Kendall, C.G.S.C. (Eds.), *Sea-level Changes: An Integrated Approach*. Society of Economic Paleontologists and Mineralogists Special Publication 42, pp. 71–108.
- Hilgen, F.J., Abdul Aziz, H., Krijgsman, W., Langereis, C.G., Lourens, L.J., Meulenkamp, J.E., Raffi, I., Steenbrink, J., Turco, E., van Vugt, N., Wijbrans, J.R., Zachariasse, W.J., 1999. Present status of the astronomical (polarity) time-scale for the Mediterranean Late Neogene. *Philos. Trans. Roy. Soc. Lond.* A357, 1931–1947.
- Ho, C.-S., 1988. An Introduction to the Geology of Taiwan: Explanatory Text of the Geology Map of Taiwan, second ed. Ministry of Economic Affairs, R.O.C., p. 192.
- Holz, M., Vilas-Boas, D.B., Troccoli, E.B., Santana, V.C., Vidigal-Souza, P.A., 2017. Chapter 4: Conceptual models of continental rift successions. In: Montenari, M., Steffensen, J.P., Singer, B., Erba, E., Raymo, M., Barker, S. (Eds.), *Stratigraphy & Timescales*, vol. 2, pp. 119–186.
- Hong, E., Wang, Y., 1988. Basin analysis of the Upper Miocene-Lower Pliocene Series in northwestern Taiwan. *Ti-Chih* 1–2, 1–22 (in Chinese).
- Holbourn, A., Kuhnt, W., Schulz, M., Flores, J.A., Andersen, N., 2007. Orbitally-paced climate evolution during the middle Miocene “Monterey” carbon-isotope excursion. *Earth Planet. Sci. Lett.* 261, 534–550.
- Huang, C.-Y., Cheng, Y.-M., 1983. Oligocene and Miocene planktonic foraminiferal biostratigraphy of northern Taiwan. *Proc. Geol. Soc. China* 26, 21–56.
- Huang, C.-Y., 1989. Implication of the Post-Lushanian faunal change for the occurrence of Kuroshio current in the early Late Miocene: Foraminiferal evidence from the Chuhuankeng section, northern Taiwan. *Proc. Geol. Soc. China* 32, 21–45.
- Huang, C.-Y., Yuan, P.B., 1996. Core analysis of the Oligocene Sandstone in the Central Uplift Zone of the Tainan Basin. Technical Report, Chinese Petroleum Corporation, Taiwan (in Chinese).
- Huang, L., 1997. Calcareous nannofossil biostratigraphy in the Pearl River Mouth Basin, South China Sea, and Neogene reticulofenestrid coccoliths size distribution pattern. *Mar. Micropaleontol.* 32, 31–57.
- Huang, T.-C., 1976. Neogene calcareous nannoplankton biostratigraphy viewed from the Chuhuankeng section, northwestern Taiwan. *Proc. Geol. Soc. China* 19, 7–24.
- Huang, T.-C., 1978. Calcareous nannoplankton, paleoenvironment, age and correlation of the upper Wulai Group and the lower Hsichih Group (Oligocene to Miocene) in northern Taiwan. *Proc. Geol. Soc. China* 21, 105–120.
- Huang, T.-C., 1979a. A supplementary note on the calcareous nannofossil, age and correlation of the Wuchihshan Formation. *Petrol. Geol. Taiwan* 16, 85–93.
- Huang, T.-C., 1979b. Calcareous nannofossil assemblage from the Nanchuang Formation and its stratigraphic significance. *Ti-Chi* 2, 13–18 (in Chinese).
- Huang, T.-C., 1980. Oligocene to Pleistocene calcareous nannofossil biostratigraphy of the Hsuehshan Range and Western Foothills in Taiwan. *Geol. Paleontol. Southeast Asia* 21, 191–210.
- Huang, T.-C., 1982. Tertiary calcareous nannofossil stratigraphy and sedimentation cycles in Taiwan. In: Salivar-Sali, A. (Ed.), *Proceedings of the Second ASCOPE Conference and Exhibition*, pp. 837–886.
- Huuse, M., Clausen, O.R., 2001. Morphology and origin of major Cenozoic sequence boundaries in the eastern North Sea Basin: Top Eocene, near-top Oligocene and the mid-Miocene unconformity. *Basin Res.* 13, 17–41.
- Juang, W.-S., 1996. Geochronology and geochemistry of basalts in the Western Foothills, Taiwan. *Bull. Natl. Museum Natl. Sci.* 7, 45–98 (in Chinese).
- Kamola, D.L., Van Wagoner, J.C., 1995. Stratigraphy and facies architecture of parasequences with examples from the Spring Canyon Member, Blackhawk Formation, Utah. In: van Wagoner, J.C., Bertram, G.T. (Eds.), *Sequence Stratigraphy of Foreland Basin Deposits – Outcrop and Subsurface Examples from the Cretaceous of North America*. American Association Petroleum Geologists Memoir 64, pp. 27–54.
- Kerr, D., Ye, L., Bahar, A., Kelkar, B.G., Montgomery, S., 1999. Glenn Pool field, Oklahoma: A case of improved prediction from a mature reservoir. *Am. Assoc. Pet. Geol. Bull.* 83, 1–18.
- Leckie, D.A., Wallace-Dudley, K.E., Vanbeselaere, N.A., James, D.P., 2004. Sedimentation in a low-accommodation setting: Nonmarine (Cretaceous) Mannville and marine (Jurassic) Ellis Groups, Manyberries Field, southeastern Alberta. *Am. Assoc. Pet. Geol. Bull.* 88, 1391–1418.
- Lee, C.-W., Chiou, T.-Y., Wu, Y.-L., 1991. Foraminiferal paleoecology and depositional model for the Oligocene of the Tainan Basin. *Rep. Explorat. Prod. Chinese Petrol. Corp.* 14, 83–102.
- Lee, C.-Y., 1994. Chronology and Geochemistry of Basaltic Rocks from Penghu Islands and Mafic Dikes from East Fujian: Implications for the Mantle Evolution of SE China since Mesozoic. Institute of Geology, National Taiwan University, PhD thesis (in Chinese).
- Lee, T.-Y., Tang, C.-H., Ting, J.-S., Hsu, Y.-Y., 1993. Sequence stratigraphy of the Tainan Basin, offshore southwestern Taiwan. *Petrol. Geol. Taiwan* 28, 119–158.
- Lin, A.T., Watts, A.B., Hesselbo, S.P., 2003. Cenozoic stratigraphy and subsidence history of the South China Sea margin in the Taiwan region. *Basin Res.* 15, 453–478.

- Martini, E., 1971. Standard Tertiary and Quaternary calcareous nannoplankton zonation. In: Farinacci, A. (Ed.), *Proceedings of the Second Planktonic Conference, Roma, 1970*, Edizioni Tecnoscienza Roma, pp. 739–785.
- Martins-Neto, M.A., Catuneanu, O., 2010. Rift sequence stratigraphy. *Mar. Pet. Geol.* 27, 247–253.
- Miller, K.G., Fairbanks, R.G., Mountain, G.S., 1987. Tertiary oxygen isotope synthesis, sea level history, and continental margin erosion. *Paleoceanography* 2, 1–19.
- Miller, K.G., Mountain, G.S., Browning, J.V., Kominz, M., Sugarman, P.J., Christie-Blick, N., Katz, M.E., Wright, J.D., 1998. Cenozoic global sea level, sequences, and the New Jersey transect: Results from coastal plain and continental slope drilling. *Rev. Geophys.* 36, 569–601.
- Plint, A. G., 1988. Sharp-based shoreface sequences and “offshore bars” in the Cardium Formation of Alberta: their relationship to relative changes in sea level. In: Wilgus, C.K., Hastings, B.S., Ross, C.A., Posamentier, H.W., van Wagoner, J., Kendall, C.G.S.C. (Eds.), *Sea-level Changes: An Integrated Approach*. Society of Economic Paleontologists and Mineralogists Special Publication 42, pp. 357–370.
- Plint, A.G., Nummedal, D., 2000. The falling stage systems tract: Recognition and importance in sequence stratigraphic analysis. In: Hunt, D., Gawthorpe, R. (Eds.), *Sedimentary Responses to Forced Regressions*, 172. Geological Society of London Special Publication, pp. 1–17.
- Posamentier, H.W., Vail, P.R., 1988. Eustatic controls on clastic deposition II: Sequence and systems tract models. In: Wilgus, C.K., Hastings, B.S., Ross, C.A., Posamentier, H. W., van Wagoner, J., Kendall, C.G.S.C. (Eds.), *Sea-level Changes: An Integrated Approach*. Society of Economic Paleontologists and Mineralogists Special Publication 42, pp. 125–154.
- Posamentier, H.W., Allen, G.P., James, D.P., Tesson, M., 1992. Forced regressions in a sequence stratigraphic framework – concepts, examples, and exploration significance. *Am. Assoc. Petrol. Geologists Bull.* 76, 1687–1709.
- Ravnas, R., Steel, R.J., 1998. Architecture of marine rift-basin successions. *Am. Assoc. Petrol. Geologists Bull.* 82, 110–146.
- Renne, P.R., Deino, A.L., Walter, R.C., Turrin, B.D., Swisher III, C.C., Becker, T.A., Curtis, G.H., Sharp, W.D., Jaouni, A.-R., 1994. Intercalibration of astronomical and radioisotopic time. *Geology* 22, 783–786.
- Selley, R.C., 1995. *Ancient Sedimentary Environments, and their Subsurface Diagnosis*, fourth ed. Chapman & Hall, p. 303 pp.
- Shanley, K.W., McCabe, P.J., 1993. Alluvial architecture in a sequence stratigraphic framework: A case history from the Upper Cretaceous of southern Utah, U.S.A. In: Flint, S., Bryant, I. (Eds.), *Quantitative Modeling of Clastic Hydrocarbon Reservoirs and Outcrop Analogues*, 15. International Association of Sedimentologists Special Publication, pp. 21–55.
- Shanley, K.W., McCabe, P.J., 1994. Perspectives on the sequence stratigraphy of continental strata. *Am. Assoc. Petrol. Geologists* 78, 544–568.
- Shaw, C.-L., 1996. Stratigraphic correlation and isopach maps of the western Taiwan basins. *Terrestrial Atmos. Oceanic Sci.* 7, 333–360.
- Sun, S.-C., 1982. The Tertiary basins of offshore Taiwan. In: Salivar-Sali, A. (Ed.), *Proceedings of the Second ASCOPE Conference and Exhibition*, pp. 125–135.
- Tai, P.-C., Lin, W.-L., Teng, L.S., 1994. Depositional environment of the Wuchihshan Formation, northern coastal Taiwan. *Ti-Chih* 14, 129–156 (in Chinese).
- Tai, P.-C., Teng, L.S., 1994. Sequence stratigraphic analysis of the Oligocene strata, northern Taiwan. *J. Geol. Soc. China* 37, 607–640.
- Teng, L.S., 1990. Geotectonic evolution of late Cenozoic arc-continent collision in Taiwan. *Tectonophysics* 183, 57–76.
- Teng, L.S., Wang, Y., Tang, C.-H., Huang, C.-Y., Huang, T.-C., Yu, M.-S., Ke, A., 1991. Tectonic aspects of the Paleogene depositional basin of northern Taiwan. *Proc. Geol. Soc. China* 34, 313–336.
- Teng, L.S., Lin, A.T., 2004. Cenozoic tectonics of the China continental margin: Insights from Taiwan. In: Malpas, J., Fletcher, C.J., Aitchinson, J.C., Ali, J. (Eds.), *Aspects of the Tectonic Evolution of China*. Geological Society, London, Special Publications, 226, pp. 313–332.
- Tensi, J., Mouthereau, F., Lacombe, O., 2006. Lithospheric bulge in the West Taiwan Basin. *Basin Res.* 18, 277–299.
- Tzeng, J., Uang, Y.-C., Hsu, Y.-Y., Teng, L.S., 1996. Seismic stratigraphy of the Tainan Basin. *Petrol. Geol. Taiwan* 30, 281–308 (in Chinese).
- Van Wagoner, J.C., Mitchum, R.M., Campion, K.M., Rahmanian, V.D., 1990. *Siliciclastic Sequence Stratigraphy in Well Logs, Cores, and Outcrops*. Am. Assoc. Petrol. Geologists Methods Exploration Ser. 7, 55 pp.
- Van Wagoner, J.C., 1995. Sequence stratigraphy and marine to nonmarine facies architecture of foreland basin strata, Book Cliffs, Utah, U.S.A. In: Van Wagoner, J.C., Bertram, G.T. (Eds.), *Sequence Stratigraphy of Foreland Basin Deposits – Outcrop and Subsurface Examples from the Cretaceous of North America*. American Association Petroleum Geologists Memoir 64, pp. 137–223.
- Van Wagoner, J.C., Posamentier, H.W., Mitchum, R.M., Vail, P.R., Sarg, J.F., Loutit, T.S., Hardenbol, J., 1988. An overview of the fundamentals of sequence stratigraphy and key definitions. In: Wilgus, C.K., Hastings, B.S., Kendall, C.G.S.C., Posamentier, H. W., Ross, C.A., van Wagoner, J.C. (Eds.), *Sea-Level Changes: An Integrated Approach*. Society of Economic Paleontologists and Mineralogists Special Publication 42, pp. 39–45.
- Vincent, E., Berger, W.H., 1985. Carbon dioxide and polar cooling in the Miocene: The Monterey hypothesis. In: Sundquist, E.T., Broecker, W.S. (Eds.), *The Carbon Cycle and Atmospheric CO<sub>2</sub>: Natural Variations, Archean to Present*. Geophysics Monograph Series 32, pp. 455–468.
- Wan, S., Kurschner, W.M., Clift, P.D., Li, A., Li, T., 2009. Extreme weathering/erosion during the Miocene Climatic Optimum: Evidence from sediment record in the South China Sea. *Geophys. Res. Lett.* 36, L19706. <https://doi.org/10.1029/2009GL040279>.
- White, N., McKenzie, D.P., 1988. Formation of the “Steers Head” geometry of sedimentary basins by differential stretching of the crust and mantle. *Geology* 16, 250–253.
- Wu, J.-C., 1991. Tectonic evolution and hydrocarbon accumulation in the Tainan Basin. *Rep. Explor. Prod.* 14, 66–82 (in Chinese).
- Yu, H.-S., Chou, Y.-W., 2001. Characteristics and development of the flexural forebulge and basal unconformity of Western Taiwan Foreland Basin. *Tectonophysics* 333, 277–291.
- Yu, N.-T., Teng, L.S., 1995. The lithofacies and sedimentary environments of the Miocene outcrops of the Chuhuangkeng section, northwestern Taiwan. *Ti-Chih* 15, 127–152 (in Chinese).
- Yu, N.-T., Teng, L.S., 1996. Facies characteristics and depositional cycles of middle and upper Miocene strata of the Western Foothills, northern Taiwan. *Ti-Chih* 15, 29–60 (in Chinese).
- Yu, N.-T., 1997. Sequence stratigraphy of the Middle to Upper Miocene strata, northern Taiwan: A preliminary study. *J. Geol. Soc. China* 40, 685–707.
- Yu, N.-T., Teng, L.S., 1998. Depositional environments of the Taliao and Shihti Formations, northern Taiwan. *Bull. Central Geol. Surv.* 12, 1–23 (in Chinese).
- Yu, N.-T., Teng, L.S., Tai, P.-C., Yue, L.-F., 1999. Relative sea-level changes in Oligocene to Miocene strata in northern Taiwan: A preliminary study. *J. Geol. Soc. China* 42, 189–208.
- Yu, N.-T., Teng, L.S., Chen, W.-S., Yue, L.-F., Chen, M.-M., 2013. Early post-rift sequence stratigraphy of a Mid-Tertiary rift basin in Taiwan: Insights into a siliciclastic fill-up wedge. *Sed. Geol.* 286–287, 39–57.
- Zachos, J., Pagani, M., Sloan, L., Thomas, E., Billups, K., 2001. Trends, rhythms, and aberrations in global climate 65 Ma to present. *Science* 292, 686–693.
- Zeccin, M., Mellere, D., Roda, C., 2006. Sequence stratigraphy and architectural variability in growth fault-bounded basin fills: A review of Plio-Pleistocene stratal units of the Crotona Basin, southern Italy. *J. Geol. Soc.* 163, 471–486.